



Inhibition Resolves Simon Conflict: Evidence From Electroencephalogram Decoding

Yoon Seo Lee¹, Gi-Yeul Bae², and Yang Seok Cho¹

Abstract

■ The congruency sequence effect, a hypothesized marker of top-down cognitive control, refers to a reduced congruency effect after incongruent trials compared with congruent trials. Although this effect has been observed across various distractor interference tasks, the nature of the control processes underlying the congruency sequence effect remains a topic of active debate. It has been suggested that cognitive control may resolve conflicts in information processing either by (a) enhancing the representation of goal information and/or (b) suppressing the representation of distractor information. The present study aimed to identify the conflict resolution processes within the context of the color Simon task by decoding the goal and distracting information from human scalp

EEG signals. For the decoding analysis, models were trained separately for color and location attributes corresponding to goal and distractor information. In addition, decoding accuracy was calculated in different frequency bands: theta (4–8 Hz), alpha (8–12 Hz), low beta (12–20 Hz), and high beta (20–30 Hz). Results showed that decoding accuracy for distractor information was reduced when cognitive control was activated, and this pattern was only observed in the high beta-frequency band (20–30 Hz). In contrast, no such difference was observed for target information. These findings suggest that cognitive control regulates Simon conflict by inhibiting distractor representation in the brain, thereby preventing unwanted distraction-driven behaviors. ■

MECHANISM OF SIMON CONFLICT RESOLUTION: EVIDENCE FROM EEG DECODING

Cognitive control refers to the ability to regulate one's thoughts and behaviors to adapt to external environmental demands or internal goals. It encompasses three key components: working memory, which enables information retention; set-shifting, which allows flexible attention shifts; and inhibition (or facilitation), which helps suppress automatic or dominant responses (Miyake et al., 2000). Among these components, inhibition is particularly crucial for self-regulation, as it allows individuals to override impulsive or habitual responses and stay focused on their goals (Diamond, 2013). Without inhibition, individuals are more likely to be driven by impulses, established habits, and environmental stimuli, leading to behavioral challenges and learning disabilities (Munakata et al., 2011). A comprehensive understanding of the mechanisms underlying inhibition is thus critical not only for improving clinical interventions but also for advancing insights into complex intelligent behavior.

One way to examine inhibition is using distractor interference tasks, where participants are required to make a novel response to a goal (task-relevant features) in the presence of a distractor (task-irrelevant features) that is strongly associated with a habitual response (Miyake et al.,

2000)—for example, in the Simon task, where participants are asked to respond to a target's color, which is presented to either the left or right of a fixation cross, while ignoring its location. Typically, performance becomes slower and less accurate when the stimulus position and the correct response location are incongruent than when they are congruent, a phenomenon known as the congruency effect. Importantly, this *congruency effect* is reduced after experiencing incongruent trials compared with congruent trials (Gratton, Coles, & Donchin, 1992)—a phenomenon called the *congruency sequence effect* (CSE; Figure 1). The robustness of the CSE has been demonstrated across various distractor interference tasks, including the Simon task (Lim & Cho, 2021b; Lee & Cho, 2013; Notebaert & Verguts, 2008; Stürmer, Leuthold, Soetens, Schröter, & Sommer, 2002), the Stroop task (Notebaert, Gevers, Verbruggen, & Liefooghe, 2006; Egner & Hirsch, 2005; Kerns et al., 2004), the flanker compatibility task (Lim & Cho, 2018; Kim & Cho, 2014), and the prime-probe task (Grant & Weissman, 2023; Grant, Cookson, & Weissman, 2020).

According to the conflict monitoring theory, the CSE arises as a consequence of enhanced top-down cognitive control following the detection of conflict in the preceding trial (Botvinick, Braver, Barch, Carter, & Cohen, 2001). Specifically, after experiencing an incongruent trial, the cognitive system adaptively modulates information processing to optimize performance on subsequent trials. This conflict monitoring process has been supported by

¹Korea University, ²Arizona State University

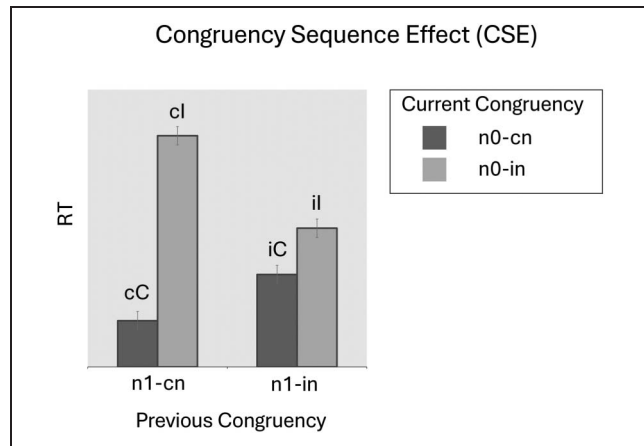


Figure 1. The diagram illustrates the CSE. The first two bars represent trials where the previous congruity was congruent, whereas the second two bars represent trials where the previous congruity was incongruent. In each set, the dark bars correspond to current congruent trials, and the light bars correspond to current incongruent trials. This creates four conditions: cC (congruent after congruent), cI (incongruent after congruent), iC (congruent after incongruent), and iI (incongruent after incongruent). “n1-cn” refers to the previous congruent trial, “n1-in” refers to the previous incongruent trial, “n0-cn” refers to the current congruent trial, and “n0-in” refers to the current incongruent trial. The CSE is characterized by current trial interference reduced after experiencing interference trials. For example, responses are typically slower for incongruent trials compared with congruent trials. However, this effect is modulated by the congruity of the previous trial. Specifically, the distraction caused by current incongruent trials is diminished after experiencing incongruent trials compared with congruent ones (i.e., iI vs. cI), reflecting the effects of conflict resolution.

neuroimaging studies (Kerns et al., 2004; MacDonald, Cohen, Stenger, & Carter, 2000; Botvinick, Nystrom, Fissell, Carter, & Cohen, 1999). fMRI research suggests that the ACC serves as the primary site for conflict detection (Botvinick et al., 1999), whereas subsequent cognitive control adjustments are mediated by the dorsolateral prefrontal cortex (DLPFC; Kerns et al., 2004; MacDonald et al., 2000). Thus, when response conflict arises during an incongruent trial, ACC identifies the conflict and transmits a control signal to the DLPFC. This interaction facilitates the recruitment of cognitive control mechanisms, thereby enhancing task-specific adjustments and reducing response conflict on subsequent trials.

Whereas the top-down cognitive control accounts effectively explain the CSE, alternative views suggest that the CSE may stem from bottom-up factors, such as stimulus and response feature-repetition priming (Hommel, Proctor, & Vu, 2004; Mayr, Awh, & Laurey, 2003) or contingency learning between task-irrelevant stimulus feature and their frequently associated responses (Schmidt & De Houwer, 2011). Nonetheless, a number of studies have consistently reported CSEs, even when both repetition-priming and contingency-learning confounds were controlled (Lim & Cho, 2021a; Kim & Cho, 2014; Schmidt &

Weissman, 2014), indicating that top-down cognitive control significantly contributes to the observed CSE.

An important question regarding top-down cognitive control in the CSE is how exactly the cognitive control in the brain operates to resolve conflicts. According to the dual-route model, information processing in the Simon task occurs along two different routes (De Jong, Liang, & Lauber, 1994; Kornblum, Hasbroucq, & Osman, 1990). The task-relevant feature is processed along a controlled route that intentionally links the stimulus to the required response, whereas the task-irrelevant feature is processed along an automatic route that directly activates the corresponding spatial responses. The overall decision is then based on a merger of both information sources (Pashler, 1997). Thus, response conflict arises when task-relevant and task-irrelevant information activate different responses. To resolve the conflict, cognitive control may operate in two possible ways: (a) by facilitating information processing through the controlled route and/or (b) by inhibiting information processing through the automatic route (Koob, Mackenzie, Ulrich, Leuthold, & Janczyk, 2023).

Notebaert and Verguts (2008) support the facilitation account, demonstrating that the scope of the Simon-type CSE is determined by the task-relevant dimension. They found that the CSE transferred across two Simon-type tasks only when both tasks shared the same task-relevant dimension (i.e., when participants responded to orientation in both tasks) and not when the tasks involved different task-relevant dimensions (i.e., responding to color in one task and orientation in the other). Thus, the authors suggested that after an incongruent trial, cognitive control enhances attention to the perceptual features of the target, thereby reducing the impact of distractions (Notebaert & Verguts, 2008; Egner & Hirsch, 2005). Conversely, others have supported the inhibition account (Lee & Cho, 2023; Stürmer et al., 2002). Stürmer and colleagues analyzed lateralized readiness potentials in the Simon task and observed early location-based priming effects over motor cortex only after congruent trials, but not after incongruent trials. They suggested that after incongruent trials, response suppression is engaged to prevent the transmission of spatial codes from the automatic route to the response output, thereby reducing the influence of task-irrelevant stimulus information. Although these studies provide important insights into the nature of cognitive control processes, RTs and averaged evoked potentials mainly reflect the consequence of control processes rather than directly revealing how the brain modulates task-relevant and task-irrelevant information.

One possible way to address this issue is to use methods that directly measure the brain representation of task-relevant and task-irrelevant information. EEG-based decoding is a novel statistical approach that used machine learning to analyze signal distributions across the scalp, providing insights into how the strength of information representation in the brain dynamically changes over time

during task performance (Fahrenfort, van Driel, van Gaal, & Olivers, 2018). Research suggested that various stimulus attributes can be decoded, including orientation (Bae & Luck, 2018), spatial location (Fahrenfort et al., 2018), color (Bae & Chen, 2024), and facial features (Bae, 2020). Moreover, recent research showed that the decoding of stimulus attributes in the current trial can vary based on previous trials (Bae, 2020; Bae & Luck, 2019). For instance, Bae and Luck (2019) demonstrated that information from preceding trials can be reactivated. They found that the orientation of a prior stimulus was decoded on the current trials. Similarly, Bae (2020) found that information from a previous trial influenced the perception of face identity and expression in the current trial, with decoding accuracy for the prior face identity increasing shortly after the current stimulus onset. These findings suggest that EEG-based decoding captures not only stimulus attributes on the current trial but also the stimulus attributes that were influenced by previous experience.

In the present study, we aimed to decode the human scalp EEG recordings of both task-relevant and task-irrelevant stimulus information following congruent and incongruent trials to examine the nature of cognitive control process. Specifically, we examined whether conflict resolution in the Simon task arises from enhanced processing of task-relevant stimulus information or from the suppression of task-irrelevant stimulus information. Participants were instructed to perform horizontal and vertical color Simon tasks alternatively in a trial-by-trial manner. Decoding analysis involved training separate models to decode color and location information for task-relevant and task-irrelevant stimulus attributes, respectively. We hypothesized that if conflict resolution enhances the processing of goal-related information, decoding accuracy for task-relevant stimulus attributes will improve following incongruent trials compared with congruent trials. Conversely, if conflict resolution suppresses distractor processing, decoding accuracy for task-irrelevant stimulus attributes will decrease following incongruent trials compared with congruent trials.

Moreover, as previous studies have shown that decoding in different frequency bands is linked to distinct cognitive states (Li et al., 2023; de Vries, Marinato, & Baldauf, 2021; de Vries, Savran, van Driel, & Olivers, 2019; van Driel, Ort, Fahrenfort, & Olivers, 2019), the present study calculated decoding accuracy separately for each frequency band. Numerous studies using the Simon task suggest that cognitive control is linked to theta oscillations (Wang et al., 2019; Cao, Cao, Yue, & Wang, 2017; Töllner et al., 2017; van Driel, Sligte, Linders, Elport, & Cohen, 2015; Gulbinaite, van Rijn, & Cohen, 2014; Cohen & Donner, 2013; Cohen & Ridderinkhof, 2013), whereas others have identified associations with alpha (Arnau, Brümmer, Liegel, & Wascher, 2021; Chinn, Pauker, & Golob, 2018) or beta oscillations (Beatty, Buzzell, Roberts, Voloshyna, & McDonald, 2021; van Es, Gross, & Schoffelen,

2020; Wiesman, Koshy, Heinrichs-Graham, & Wilson, 2020; Duprez et al., 2019). However, many of these studies utilized only two response alternatives (e.g., left and right keys), which could confound the results with bottom-up repetition priming. Although some studies attempted to control for these factors by excluding stimulus repeating trials from analysis, it remains unclear whether consistent results would be obtained using a paradigm specifically designed to minimize such confounds.

To investigate top-down cognitive control, the present study adopted a bottom-up confound-minimized design. Decoding accuracy was measured in theta (4–8 Hz), alpha (8–12 Hz), low beta (12–20 Hz), and high beta (20–30 Hz) frequency bands to confirm findings from this confound-minimized design. The gamma frequency band (30–100 Hz), which is primarily associated with bottom-up processing (Buschman & Miller, 2007), was excluded from the analysis, as the study focus was solely on top-down cognitive control. Finally, a general analysis of oscillatory activity was conducted to validate the decoding analysis. We hypothesized that if conflict is resolved by enhancing attention toward task-relevant color information (Notebaert & Verguts, 2008), modulation would occur in the alpha frequency band, which has been strongly associated with attentional modulation (Peylo, Hilla, & Sauseng, 2021; Schneider, Herbst, Klatt, & Wöstmann, 2022; Foster & Awh, 2019; Van Diepen, Foxe, & Mazaheri, 2019; Thut, Nietzel, Brandt, & Pascual-Leone, 2006). If Simon-type conflict is resolved by suppressing task-irrelevant location information, specifically the automatic route from task-irrelevant dimensions to response (Stürmer et al., 2002), modulation should appear in the beta frequency band, as beta oscillations are closely linked to response modulation (Schmidt et al., 2019; Spitzer & Haegens, 2017; Pavlidou, Schnitzler, & Lange, 2014; Engel & Fries, 2010). Lastly, if modulation occurs in the theta frequency band, it may imply that conflict is resolved beyond simple inhibition or facilitation, as theta oscillations have been associated with working memory (Riddle, Scimeca, Cellier, Dhanani, & D'Esposito, 2020), episodic memory (Nyhus & Curran, 2010), and episodic retrieval (Frackowiak et al., 2004).

METHODS

Participants

The sample size was determined using G*Power 3.1 (Faul, Erdfelder, Buchner, & Lang, 2009). On the basis of the experiment conducted by Lee and Cho (2023; Experiment 2), where $\eta_p^2 = .212$, a repeated-measures ANOVA was conducted to examine the two-way interaction between Previous-Trial Congruency (congruent or incongruent) and Current-Trial Congruency (congruent or incongruent). The statistical power ($1-\beta$) set at .95 and the alpha level at 5% were applied. Our estimation indicated that a minimum sample size of 26 would provide 96% power to observe a CSE between two tasks.

Thirty participants (14 female, 16 male; mean age = 23.8 years) from Korea University participated in the experiment. All participants self-reported as right-handed and no deficit in visual acuity or color vision. Before the experiment, all participants provided informed consent and received compensation of KRW 50,000 (about \$37) after their participation. The experiment was approved by the institutional review board of Korea University (KU-IRB-16-142-A-1).

Stimuli and Apparatus

The experiment was conducted using MATLAB software (Version 2015a; The MathWorks) and the Psychophysics Toolbox Version 3. Visual stimuli were presented on a 24-in. (16:9) LCD monitor positioned approximately 55 cm from the participants. The sequence of displays and time course for the Simon tasks are illustrated in Figure 2A. A white (red [R] = 255, green [G] = 255, blue [B] = 255) cross served as the fixation point, appearing at the center of the display. The experiment consists of vertical and horizontal Simon tasks. For the horizontal

Simon task, a blue (R = 0, G = 0, B = 255) or yellow (R = 255, G = 255, B = 0) square (approximately $1.51^\circ \times 1.51^\circ$) was presented to either the left side or right side of the fixation cross. For the vertical Simon task, a red (R = 255, G = 0, B = 0) or green (R = 0, G = 255, B = 0) square was presented either above or below the fixation cross. The target stimulus appeared at an equal distance from the center of the display (approximately 5.4°). All stimuli were displayed on the gray background (R = 128, G = 128, B = 128).

Responses were recorded with a standard 101-key computer keyboard. The “4,” “6,” “8,” and “2” keys on the numeric keypad were used as directional responses, indicating “left,” “right,” “up,” and “down,” respectively. The “5” key or home key was used as the starting position.

Task Design

A confound minimized design was employed (Lim & Cho, 2021a; Kim & Cho, 2014; Schmidt & Weissman, 2014). To avoid bottom-up feature integration, horizontal and vertical color Simon tasks were alternated in a trial-by-trial manner (Figure 2A). Horizontal stimulus (i.e., blue and yellow)

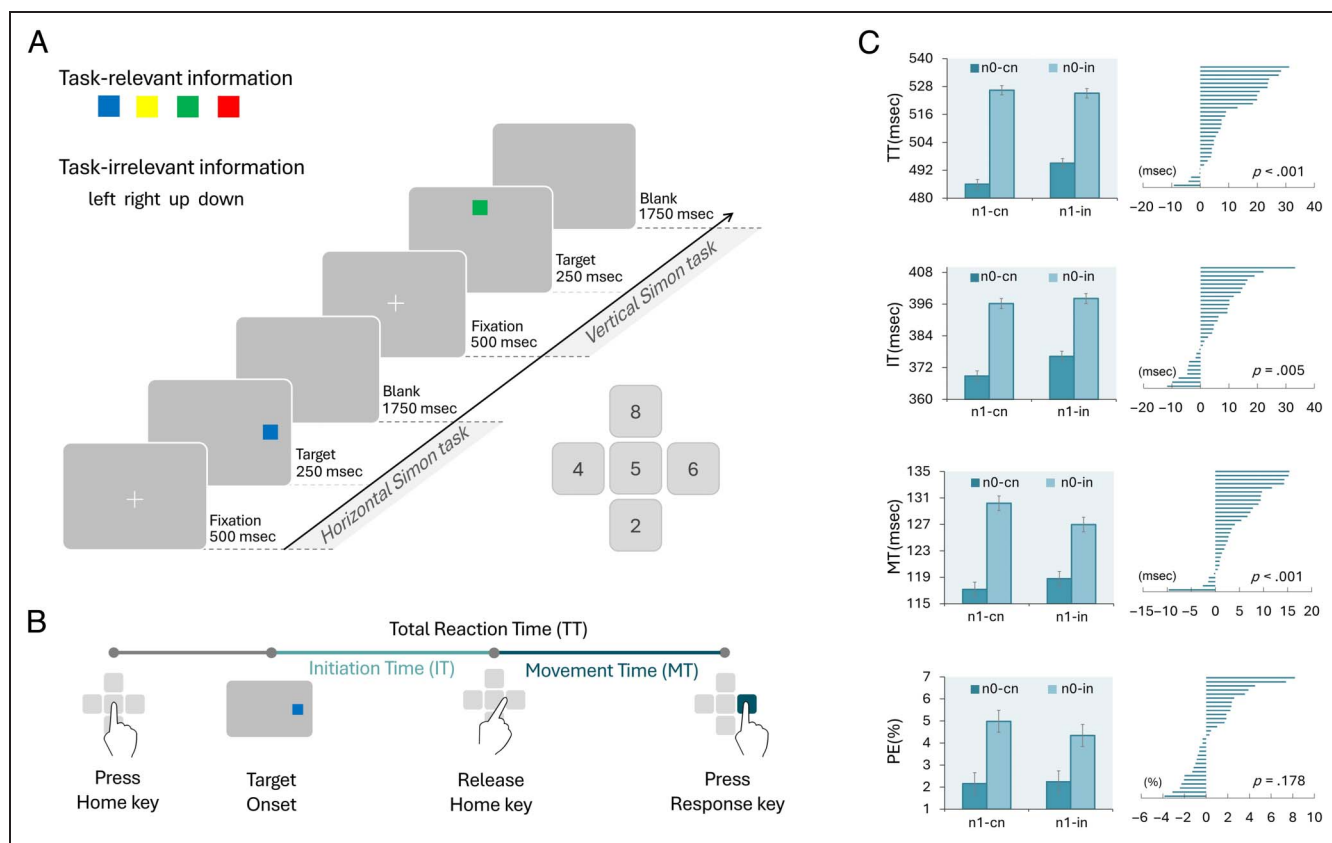


Figure 2. Task paradigm and behavioral results. (A) An example of task sequence and response keys. Horizontal and vertical Simon tasks were presented alternatively in a trial-by-trial manner. Participants were asked to respond to the color of the square while ignoring the location of the square. Thus, the task-relevant information was color (blue, yellow, green, and red), and the task-irrelevant information was location (left, right, up, and down). (B) A diagram for response method. Participants were instructed to keep pressing the home key and release it when they decided their response. Once they release the home key, they were asked to press a response key. TT was separated into IT and MT. IT is the temporal duration from the target onset to the release of the home key. MT is the duration from the release of the home key to the pressing of an actual response key. (C) Behavioral results of TT, IT, MT, and PEs. Left: Bar graphs for the averaged data for the four conditions (i.e., cC, cl, iC, and iI). Right: CSE, calculated as $(cI - cC) - (iI - iC)$, for individual participants.

and response sets (i.e., left and right) were presented in odd trials, whereas vertical stimulus (i.e., red and green) and response sets (i.e., up and down) were presented in even trials, thereby preventing stimulus and response repetition in consecutive trials. To avoid contingency learning confounds, eight unique stimuli (i.e., blue-left, blue-right, yellow-left, yellow-down, red-up, red-down, green-up, green-down) were presented exactly 10 times in each block.

To ensure that the horizontal and vertical dimensions of the stimulus and response were equally salient during the Simon task, we adopted the aimed-movement response method proposed by Lim and Cho (2021b). The “4” and “6” keys were used as directional keys for the horizontal Simon task, whereas the “8” and “2” keys were used for the vertical Simon task. To maintain consistency across the spatial dimensions, all responses started from the “5” home key. Participants were instructed to keep pressing the home key until they had decided on their response. Once they made their decision, they pressed the corresponding directional key and then returned to the home key.

This method provides an advantage over conventional RT measures by allowing total RT (TT) to be decomposed into initiation time (IT) and movement time (MT) for a more refined examination. IT is defined as the time from the target onset to the moment the home key is released, whereas MT is the time from home key release to pressing the directional key. If a CSE is observed in IT, it suggests that conflict resolution occurs at an earlier stage of information processing (e.g., stimulus identification to response selection). In contrast, if a CSE appears in MT, it implies that conflict resolution takes place at a later stage (e.g., movement execution).

However, the distinction between response selection and execution is not always clear-cut, and some studies suggest that these processes may overlap, allowing responses to be initiated even before response selection is fully completed (Lee & Cho, 2024; Calderon, Gevers, & Verguts, 2018; Buetti & Kerzel, 2008, 2009; Hommel, 2009; Resulaj, Kiani, Wolpert, & Shadlen, 2009; Erlhagen & Schöner, 2002). Therefore, although separating IT and MT provides insights into the temporal dynamics of conflict resolution, it does not provide absolute evidence that these stages are functionally independent. In particular, IT may not accurately reflect the speed of response selection if the response selection is still executed during the response execution period despite participants being instructed to release the home key only after deciding on their response. To mitigate this issue, our study incorporated the methods developed in previous studies (Rubichi & Pellicano, 2004; Smith & Carew, 1987). In the task, the target stimulus disappeared immediately upon home key release, motivating participants to delay movement initiation until response selection was completed (Smith & Carew, 1987). In addition, in the analyses, trials with extreme deviations in either IT or MT were excluded

because RT measures in those trials might be conflated by the trade-offs between response selection and response execution. For similar reasons, trials in which MT was longer than IT and trials where the home key was released before target onset were removed as errors. These methods ensured that IT and MT more accurately reflect the speed of response selection and response execution.

Counterbalancing was implemented to ensure that decoding focused exclusively on task-relevant color attributes, without being influenced by specific response associations. Furthermore, because neuroimaging data can be highly variable across individuals due to anatomical, functional, and cognitive differences (Dubois & Adolphs, 2016), counterbalancing was employed within participants. This approach ensured that each participant experienced different stimulus-response (S-R) mappings, thereby controlling for individual differences and increasing the sensitivity to detect true effects. Thus, participants completed the tasks twice, with a week between sessions, each session with different S-R mappings (i.e., blue-left, yellow-right, red-up, green-down, or blue-right, yellow-left, red-down, green-up). The order of S-R mappings varied across participants. To minimize potential confounding factors, each session was conducted on the same day of the week (e.g., every Monday), at the same time (e.g., at 2 p.m.), and under the same environmental conditions.

Procedure

After providing informed consent, participants performed the tasks in a dimly lit sound-proof chamber. The participant's body midline and the numeric keypad were aligned with the center of the monitor. Participants were instructed to press one of the directional response keys on the numeric keypad depending on the color of the target stimulus as quickly and accurately as possible. The instructions also informed of the four S-R mappings. On each trial, when the fixation cross was presented, participants were instructed to press the home key with their right index finger and to keep pressing the key until they decided their response to the target after it was presented. Five hundred milliseconds after the home key was pressed, a target stimulus was presented for 250 msec or until the home key was released. After the target display, a blank display was presented for 1750 msec. Participants were instructed to press one of the four direction keys depending on the color of the target stimulus. All responses were executed using the right index finger. If the release of the home key occurred before target presentation, a visual feedback message was displayed, saying “Press the home key.” Each time a participant responded incorrectly or failed to respond within 2000 msec after the target onset, a 150-msec beep sound was played as feedback.

After a practice block of 34 trials, participants completed eight blocks of 82 trials, with 1-min breaks between blocks. The four sequential trial types—congruent trial followed by a congruent trial (cC), congruent trial followed by an incongruent trial (cI), incongruent trial followed by a congruent trial (iC), and incongruent trial followed by an incongruent trial (iI)—were presented with equal frequency in both the horizontal and vertical Simon tasks. The congruency for the first and second trials of each block was randomly determined.

Behavior Analysis

In the behavioral analyses, the following trials were excluded: practice trials, the first two trials of each block, outliers (defined as trials that deviated by more than 3 SDs from the conditional mean for each participant), trials following an outlier, incorrect trials, trials in which MT was longer than IT, and trials where the home key was released before the target stimulus appeared. These exclusions accounted for approximately 3.28% of the total trials. Following these exclusions, the individual mean correct TTs, ITs, MTs, and percentage errors (PEs) were calculated separately for the combination of previous-trial congruency (congruent, incongruent) and current-trial congruency (congruent, incongruent). Two-way repeated-measures ANOVAs were conducted on mean TTs, ITs, MTs, and PEs with those variables as within-subject variables.

EEG Recording and Preprocessing

EEG signals were recorded using SynAmps RT NeuroScan 64-channel EEG system (NeuroScan Compumedics) with a pass-band of 0.01–200 Hz. The ground electrode was positioned between the FPz and Fz electrodes. Signals from two additional electrodes (M1 and M2) attached to the left and right earlobes were used as the reference electrodes. Eye movements were measured with VEOG and HEOG. VEOG electrodes were positioned above and below the left eye, whereas HEOG electrodes were positioned 1 cm lateral to the outer canthi of each eye. Electrocardiogram signals were recorded to exclude the effects of cardiac (ECG) signals (Park, Correia, Ducorps, & Tallon-Baudry, 2014) with two electrodes placed approximately 2 cm below the left and right collarbones. In the EEG system with 64 channels, two channels were designated as ground and reference. In addition, separate electrodes used as bipolar channels (HEOG and VEOG) for eye movement monitoring, reference electrodes (i.e., M1 and M2), and a bipolar channel for recording cardiac signals (ECG) were excluded. Channel impedances were maintained below 15 kΩ.

The preprocessing of the signals was conducted using the EEGLAB Toolbox (Delorme & Makeig, 2004) and the ERPLAB Toolbox (Lopez-Calderon & Luck, 2014). Scalp EEG signals were offline referenced to the average of the left and right earlobes. All signals were band-pass filtered

(noncausal Butterworth impulse response function, half amplitude cutoffs at 0.1 and 80 Hz, 12 dB/oct roll-off) and resampled at 250 Hz. Any EEG signals containing significant muscle artifacts or extreme voltage offsets were automatically and manually identified and removed. The independent component analysis was subsequently applied on the scalp EEG for each participant to identify and remove components associated with blinks (Jung et al., 2000) and eye movements (Drisdelle, Aubin, & Jolicœur, 2017). Following independent component analysis correction, the EEG data were segmented for each trial from −500 to +1200 msec relative to the onset of the stimulus (i.e., baseline: [−500, 0]; stimulus presentation: [0, 250]; blank: [250, 1200]). Standard artifact rejection procedures (Luck, 2014) were then implemented to eliminate epochs containing miscellaneous artifactual voltage deflection. The average percentage of rejected trials was 7.52%. After removing artifacts, the counterbalanced data for each participant were concatenated.

It has been suggested that EEG decoding is susceptible to movement-related artifacts, making it essential to control motor activity during recording (Jansen et al., 2012; Luck, 2012). Moreover, analyzing EEG signals during movement execution can reduce the signal-to-noise ratio, leading to ambiguous decoding results (Luck, 2012). Given that the primary goal of the present decoding analysis was to track the temporal dynamics of task-relevant and irrelevant information, we time-locked EEG signals to stimulus onset, focusing on the period between stimulus presentation and response execution.

Decoding

The preprocessed data set was first categorized based on the congruency of the previous trial and then further divided according to the color or location attributes of the current trial. As a result, the data set was classified into four groups: color information following a congruent trial, collapsed across locations; location information following a congruent trial, collapsed across colors; color information following an incongruent trial, collapsed across locations; and location information following an incongruent trial, collapsed across colors. Importantly, because each trial contains both color and location information, the training data for color and location remain identical within the same congruency condition. However, the key difference lies in the labeling approach. That is, although the input data remains the same, the classification targets differ, allowing the model to independently learn patterns associated with color and location. Consequently, for color decoding, trials were labeled according to the color of the presented square (e.g., blue-1, yellow-2, red-3, green-4), whereas for location decoding, trials were labeled based on the spatial position of the square (e.g., left-1, right-2, up-3, down-4).

In the decoding analysis, data were divided into two conditions (trials after congruent and trials after incongruent). Current congruency was intentionally collapsed

within the data set to avoid redundancy between the color and location data sets. If the data were divided into four conditions (cC, cI, iC, and iI), trials that are current congruent (e.g., a blue square on the left side either in cC and iC) would result in identical markings for both color and location data sets (e.g., both being labeled as "1"). This overlap would reduce the independence needed for effective analysis. To maintain a clear distinction between the color and location data sets, the data were divided based on previous congruency, while collapsing current congruency. This approach prevents the issue of identical labeling that would occur when mixing congruent and incongruent current trials. Similar methods of collapsing current congruency to focus on the effects of previous experiences have been applied in previous neuroimaging research (Pastötter, Dreisbach, & Bäuml, 2013; Fan et al., 2007).

For the decoding analysis, the Amsterdam Decoding and Modeling toolbox (Fahrenfort et al., 2018) was used on the preprocessed EEG data. Before classification, the EEG data were resampled to 50 Hz to reduce computation time. To ensure that the training of the classifier was not biased across classes, an undersampling method was applied. This involved randomly selecting trials from the conditions with more trials to balance them with the conditions having fewer trials, resulting in an equal count of subsequent congruent and subsequent incongruent trials within each class. Training and testing were performed on the same data set for each condition separately using a fivefold cross-validation procedure. The data set was divided into five equal-size groups of trials; four out of these groups were used for training, and the remaining fifth was reserved for testing. Linear discriminant analysis (LDA) classifiers were adopted for each category of information, with each classifier trained to differentiate between one attribute versus the others. For example, in color decoding, models classified one color (e.g., red) versus the other colors, whereas in location decoding, the model classified one location (e.g., left) versus the other locations. The trained models were then employed to predict the color or location of each test data point reserved for testing. This process was repeated five times until all data were tested. Classifier performance was then averaged across folds. The decoding analysis was conducted using data from all 62 scalp channels.

It is important to note that the LDA classifier is unlikely to misinterpret color signals as location signals because location attributes are mixed within each color attribute and vice versa. In addition, the LDA classifier is unlikely to decode color or location attributes based solely on horizontal or vertical information, as both dimensions are integrated within each attribute. Although some stimulus attributes are associated with specific dimensions (e.g., horizontal with blue and yellow, vertical with red and green), it is improbable that the classifier would differentiate attributes based purely on this. Even if dimensional information were used, the classifier would still need to detect distinct features within each dimension to

accurately differentiate stimulus attributes. Finally, it is unlikely that the evidence for color decoding is confounded with response decoding, given that the mapping of colors to responses was strictly counterbalanced.

The area under the curve (AUC) per time point, derived from the signal detection theory, was used as a measure of classification accuracy. *t* Tests were conducted across participants against a 50% chance level. Although the model classifies one out of four attributes, the ADAM toolbox computes AUC for multiclass problems by averaging the AUC across all pairwise comparisons between classes (Fahrenfort et al., 2018). As a result, the chance AUC performance is consistently 50%, regardless of the number of classes being analyzed. Differences in classification accuracy between previous congruent and previous incongruent conditions were then calculated for both color and location accuracy. Cluster-based permutation tests ($p < .05$, 1000 iterations) were then used to perform multiple-comparison correction for these *t* tests over time (Cohen, 2014; Maris & Oostenveld, 2007; Nichols & Holmes, 2002). The null distribution of the cluster size under random permutation was determined based on the observed cluster size, and *p* values for the clusters were calculated using this comparison. Because the neural representation of color or location starts from target onset and ends when the response is made, the analysis period for the decoding AUC was set from 0 to 600 msec. This duration was determined based on the average TT, which was 508 msec (Table 1). This AUC reflects the accuracy of machine learning in discriminating stimulus attributes, which, in other words, indicates the strength of the stimulus representation in the brain. Finally, this decoding accuracy was calculated in different frequency bands: in theta (4–8 Hz), alpha (8–12 Hz), low beta (12–20 Hz), and high beta (20–30 Hz).

Time-Frequency Analysis

Time-frequency analysis was conducted to determine whether consistent results could be observed in comparison to the decoding outcomes. The data were decomposed into frequency bands using complex Morlet wavelet convolution, following the method described by Cohen (2014). The wavelets' frequencies ranged from 2 to 40 Hz, comprising 60 linearly spaced wavelets. Complex

Table 1. Mean of TT, IT, MT, and PEs

N-1 Congruency	N-0 Congruency	TT	IT	MT	PE
Congruent	Congruent	486	368	117	2.1
	Incongruent	526	396	130	4.9
Incongruent	Congruent	495	376	118	2.2
	Incongruent	525	398	126	4.3
Average		508	384	123	3.3

Morlet wavelets were created by multiplying a Gaussian ($e^{-t^2/2s^2}$, where s is the width of the Gaussian) with sine waves ($e^{i2\pi ft}$, where i is the complex operator, f is frequency, and t is time). The Gaussian width was set as $s = \delta/(2\pi f)$, where δ represents the number of cycles of each wavelet, logarithmically spaced between 4 and 40 to have a good tradeoff between temporal and frequency precision. Frequency-domain convolution was applied, that is, applying the fast Fourier transform to both the EEG data and the Morlet wavelets, multiplying them, and converting the result back to the time domain using the inverse fast Fourier transform. The squared magnitude of these complex signals was taken at each time point and each frequency to acquire power, that is, $[\text{real}(Z_t^2) + \text{imag}(Z_t^2)]$. Power was then decibel-normalized [$\text{dB Power}_{tf} = 10 * \log_{10}(\text{Power}_{tf} / \text{Baseline Power}_f)$], where baseline is the frequency-specific average of power values over -300 to -100 prestimulus time period.

Normalized power data were averaged based on the conditions: cC, cI, iC, and ii. The calculation for condition subtraction was based on the formula: CSE = (cI - cC) - (ii - iC). Statistics were performed by one-sample t tests against zero, and multiple comparisons were corrected through cluster-based permutation testing. In the permutation test, condition labels were randomly shuffled for each data point, and t values were recomputed. The sum of t values within the largest cluster was recorded into a distribution of summed cluster t values. This process was repeated 1000 times, generating a distribution of maximum cluster sizes under the null hypothesis. Any clusters in the true data that were greater than or less than 95% of the null distribution (i.e., $p < .05$) were considered statistically significant.

Time-frequency ROI analysis was further adopted to elucidate the difference between the conditions. The time-frequency ROI windows were selected based on the location of the cluster and decoding results, with the time window set at 400–500 msec. Power was then calculated separately for the combination of Previous-Trial Congruency (congruent, incongruent) and Current-Trial Congruency (congruent, incongruent). Two-way repeated-measures ANOVAs were conducted on mean power with the above variables as within-subject variables.

The selection of electrodes was conducted independently of any potential variations across task conditions or frequency bands, ensuring an unbiased approach. First, we hypothesized that conflict resolution would most likely be observed at electrodes frequently cited in the literature for top-down conflict resolution, such as the frontocentral electrode FCz (Duprez, Gulbinaite, & Cohen, 2020; Wang, Du, Hopfinger, & Zhang, 2018; Hoppe, Küper, & Wascher, 2017; Gulbinaite et al., 2014; Cohen & Donner, 2013; van Driel, Ridderinkhof, & Cohen, 2012; Spapé et al., 2011) and the central electrode Cz (Rey-Mermet, Gade, & Steinhauser, 2019; Li et al., 2015; Tang, Hu, & Chen,

2013; Clayson & Larson, 2011; Frühholz, Godde, Finke, & Herrmann, 2011; Larson & Clayson, 2011; Chen & Melara, 2009). However, previous studies have also reported conflict resolution activity in other regions, including frontal, central-parietal, and posterior areas (Kahamala, Ociepka, & Chuderski, 2020; Eder, Leuthold, Rothermund, & Schweinberger, 2012; Chen & Melara, 2009). Because the effects related to cognitive control were observed across multiple electrode sites, we first conducted a whole-channel analysis to determine whether the observed patterns were specific to certain channels or reflected a more widespread phenomenon. This analysis included ROI analysis as well as cluster-corrected permutation tests. Moreover, the evaluation was performed in different frequency bands: theta (4–8 Hz), alpha (8–12 Hz), low beta (12–20 Hz), and high beta (20–30 Hz). The results revealed that Cz was the only electrode to exhibit a significant CSE and confirmed by cluster-corrected permutation testing. As a result, FCz was excluded from further analysis, and Cz was selected for subsequent time-frequency analyses. The lack of significant differences at FCz may be attributed to individual anatomical differences (Ignatiadis, Barumerli, Tóth, & Baumgartner, 2022) or ethnic variations in cranial shape, such as brachycephaly (short-headed) and dolichocephaly (long-headed; Ball et al., 2010), which could cause slight variations in vertical electrode placement.

RESULTS

Behavioral Results

Total Time (TT)

The main effect of Previous-Trial Congruency was significant, $F(1, 29) = 9.59, p = .004$, mean squared error (MSE) = 46, $\eta_p^2 = .248$, with the mean TT significantly greater after incongruent trials ($M = 510$ msec) than after congruent trials ($M = 506$ msec). A significant Simon effect was observed, as the main effect of Current-Trial Congruency was significant, $F(1, 29) = 153.14, p < .001, MSE = 242, \eta_p^2 = .840$. The mean TT was greater on incongruent trials ($M = 525$ msec) than congruent trials ($M = 490$ msec). There was a significant interaction between Previous-Trial Congruency and Current-Trial Congruency, $F(1, 29) = 27.91, p < .001, MSE = 28, \eta_p^2 = .490$, indicating a CSE (Figure 2C). The magnitude of the Simon effect was reduced after incongruent trials (30 msec), $F(1, 29) = 124.91, p < .001, MSE = 108, \eta_p^2 = .811$, compared with after congruent trials (40 msec), $F(1, 29) = 149.72, p < .001, MSE = 163, \eta_p^2 = .837$. To test whether distractor interference was reduced, we conducted a one-way ANOVA with Previous-Trial Congruency (congruent, incongruent) as a within-subject variable, focusing on trials where the current trial was incongruent (i.e., the difference between cI and ii). The analysis revealed no significant difference between the cI and ii conditions, $F(1, 29) < 1$.

Initiation Time (IT)

The main effect of Previous-Trial Congruency was significant, $F(1, 29) = 18.03, p = .002, MSE = 36, \eta_p^2 = .383$, with the mean IT significantly greater after incongruent trials ($M = 387$ msec) than after congruent trials ($M = 382$ msec). The main effect of Current-Trial Congruency was significant, $F(1, 29) = 111.62, p < .001, MSE = 162, \eta_p^2 = .793$. The mean IT was greater on incongruent trials ($M = 397$ msec) than congruent trials ($M = 372$ msec). The interaction between previous-trial congruency and current-trial congruency was significant, $F(1, 29) = 8.87, p = .005, MSE = 25, \eta_p^2 = .234$ (Figure 2C). The magnitude of the Simon effect was reduced after incongruent trials (21 msec), $F(1, 29) = 106.56, p < .001, MSE = 67, \eta_p^2 = .786$, compared with after congruent trials (27 msec), $F(1, 29) = 92.47, p < .001, MSE = 121, \eta_p^2 = .761$. However, the difference between cI and iI was not significant $F(1, 29) = 1.73, p = .19$. Moreover, as the iI ($M = 398$ msec) was not faster than cI ($M = 396$ msec), this is not a typical pattern of the CSE (Figure 1).

Movement Time (MT)

The main effect of Previous-Trial Congruency was marginally significant, $F(1, 29) = 3.26, p = .081, MSE = 5.85, \eta_p^2 = .101$. The mean MT was slightly lower after incongruent trials ($M = 122$ msec) than after congruent trials ($M = 123$ msec). The main effect of Current-Trial Congruency was significant, $F(1, 29) = 60.36, p < .001, MSE = 55, \eta_p^2 = .675$. The mean MT was greater on incongruent trials ($M = 128$ msec) than congruent trials ($M = 117$ msec). The interaction between previous-trial congruency and current-trial congruency was significant, $F(1, 29) = 19.8, p < .001, MSE = 8.8, \eta_p^2 = .405$, indicating a CSE (Figure 2C). The magnitude of the Simon effect was smaller after incongruent trials (8 msec), $F(1, 29) = 40.82, p < .001, MSE = 24, \eta_p^2 = .584$, than after congruent trials (13 msec), $F(1, 29) = 63.47, p < .001, MSE = 40, \eta_p^2 = .686$. Moreover, a significant difference was found between the cI and iI conditions, $F(1, 29) = 17.74, p < .001, MSE = 8.71, \eta_p^2 = .379$, with distractor interference significantly reduced on iI compared with cI, suggesting that conflict experience contributed to a reduction in distractor interference in the MT data.

Percentage Errors (PEs)

The main effect of Previous-Trial Congruency was not significant, $F(1, 29) = 2.14, p = .15$. The main effect of Current-Trial Congruency was significant, $F(1, 29) = 21.03, p < .001, MSE = 8.66, \eta_p^2 = .420$. PE was higher on incongruent trials (4.66%) than congruent trials (2.20%). Interaction between previous-trial congruency and

current-trial congruency was not significant, $F(1, 29) = 1.9, p = .178$ (Figure 2C).

Decoding Results

Theta (4–8 Hz)

The color decoding accuracy began to rise above chance level after the target onset and gradually decreased after reaching its peak at approximately 200 msec but remained significant for the rest of the analysis period for both after congruent (*cluster-corrected* $p < .05$) and after incongruent trials (*cluster-corrected* $p < .05$; Figure 3A left).

Similarly, the location decoding accuracy began to rise above chance level after the target onset and gradually decreased after reaching its peak at approximately 200 msec but remained significant for the rest of the analysis period for both after congruent (*cluster-corrected* $p < .05$) and after incongruent trials (*cluster-corrected* $p < .05$; Figure 3A right). However, there was no significant AUC difference between after congruent and incongruent trials in both color and location decoding ($p > .05$).

Alpha (8–12 Hz)

The color decoding accuracy began to rise above chance level after the target onset and gradually decreased after reaching its peak at approximately 200 msec but remained significant for the rest of the analysis period for both after congruent (*cluster-corrected* $p < .05$) and after incongruent trials (*cluster-corrected* $p < .05$; Figure 3B left).

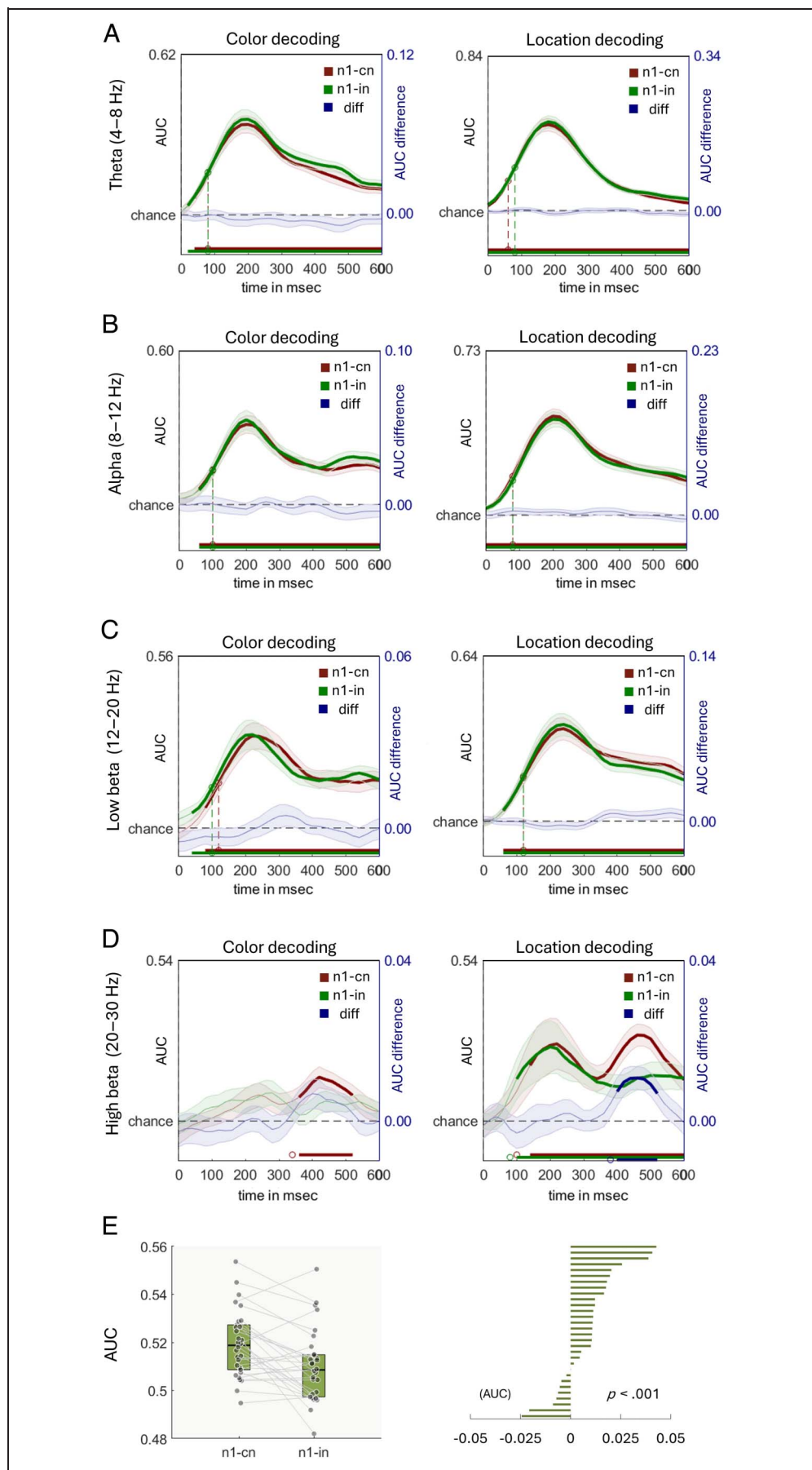
Similarly, the location decoding accuracy began to rise above the chance level after the target onset and gradually decreased after reaching its peak at approximately 200 msec but remained significant for the rest of the analysis period for both after congruent (*cluster-corrected* $p < .05$) and after incongruent trials (*cluster-corrected* $p < .05$; Figure 3B right). However, there was no significant AUC difference between after congruent and incongruent trials in both color and location decoding ($p > .05$).

Low Beta (12–20 Hz)

The color decoding accuracy began to rise above chance level after the target onset and gradually decreased after reaching its peak at approximately 250 msec but remained significant for the rest of the analysis period for both after congruent (*cluster-corrected* $p < .05$) and after incongruent trials (*cluster-corrected* $p < .05$; Figure 3C left).

Similarly, the location decoding accuracy began to rise above chance level after the target onset and gradually decreased after reaching its peak at approximately 200 msec but remained significant for the rest of the

Figure 3. Decoding results. Color and location decoding AUCs were measured from target onset to response execution across different frequency bands: (A) theta (4–8 Hz), (B) alpha (8–12 Hz), (C) low beta (12–20 Hz), and (D) high beta (20–30 Hz). Thicker lines represent time windows where classification performance was statistically significant ($p < .05$, cluster-corrected). Here, “n1-cn” means previous congruent, “n1-in” means previous incongruent, and “diff” means the accuracy differences between previous congruent and previous incongruent conditions. (E) The left figure shows location decoding accuracy of previous congruent and previous incongruent trials in high beta frequency band (20–30 Hz) from 400 to 520 msec. The right figure shows individual congruency effect (i.e., previous congruent – previous incongruent) within the selected time and frequency window.



analysis period for both after congruent (*cluster-corrected p < .05*) and after incongruent trials (*cluster-corrected p < .05*; Figure 3C right). However, there was no significant AUC difference between after congruent and incongruent trials in both color and location decoding ($p > .05$).

High Beta (20–30 Hz)

There was significant above chance color decoding that was observed in previous congruent trials (approximately from 350 msec to 505 msec, *cluster-corrected p < .05*; Figure 3D left). No other significance was observed in color decoding including the difference between previous congruent and incongruent trials.

For location decoding, after congruent trials, the accuracy began to rise above the chance level at 100 msec after the target onset and gradually decreased after reaching its peak at approximately 200 msec. The accuracy rerise and reach its peak again at approximately 480 msec and remained significant for the rest of the analysis period (*cluster-corrected p < .05*; Figure 3D right). Whereas after incongruent trials, the location decoding accuracy began to rise above the chance level at 100 msec after the target onset and gradually decreased after reaching its peak at approximately 200 msec but remained significant for the rest of the analysis period (*cluster-corrected p < .05*). Importantly, there was a significant difference between AUC after congruent and incongruent trials (from 400 msec to 520 msec, *cluster-corrected p = .017*), suggesting significantly lower decoding accuracy after incongruent trials compared with after congruent trials. To further confirm the result in the univariate analysis, we extracted data from the significant interval (i.e., from 400 msec to 520 msec) and averaged in each individual to conducted one-way ANOVA with Previous-Trial Congruency (congruent, incongruent) as a within-subject variable. We found a significant difference in Previous-Trial Congruency, $F(1, 29) = 13.83, p < .001, MSE < .001, \eta_p^2 = .322$ (Figure 3E), indicating a significant conflict modulation was observed in location decoding, particularly in high beta oscillations at 400–520 msec.

Time-Frequency Results

Theta (4–8 Hz)

Electrodes FC1, FC2, F6, and FC6 showed statistically significant condition-related differences ($p < .05$; Figure 4A). To further explore the interaction pattern, we grouped FC1 and FC2 together, as well as F6 and FC6, based on the contour lines observed in the topographical map. For the FC1 and FC2 group, the main effect of Current-Trial Congruency was not significant, $F(1, 29) < 1$. However, a significant interaction between Previous-Trial Congruency and Current-Trial Congruency was observed, $F(1, 29) =$

9.55, $p = .004, MSE = 13.12, \eta_p^2 = .247$. The difference between cI and iI was significant $F(1, 29) = 4.3, p = .047, MSE = 20.89, \eta_p^2 = .129$. Similarly, for the F6 and FC6 group, the main effect of Current-Trial Congruency was not significant, $F(1, 29) < 1$, but a significant interaction between Previous-Trial Congruency and Current-Trial Congruency was found, $F(1, 29) = 5.73, p = .023, MSE = 9.81, \eta_p^2 = .165$. The difference between cI and iI was not significant $F(1, 29) < 1$. As depicted in Figure 4A, both interactions did not follow the typical pattern of the CSE (Figure 1). Furthermore, no significant clusters were found in any of the electrodes.

Alpha (8–12 Hz)

Electrode Cz exhibited statistically significant condition-related differences ($p < .05$; Figure 4B). The main effect of Current-Trial Congruency was not significant, $F(1, 29) < 1$. However, a significant interaction between Previous-Trial Congruency and Current-Trial Congruency was observed, $F(1, 29) = 5.68, p = .023, MSE = 19.16, \eta_p^2 = .163$. The difference between cI and iI was significant $F(1, 29) = 7.11, p = .012, MSE = 21.17, \eta_p^2 = .197$. As shown in Figure 4B, this interaction did not follow the typical pattern of the CSE (Figure 1). Furthermore, no significant clusters were found in the alpha frequency domain.

Low Beta (12–20 Hz)

Electrodes C5 and P8 exhibited statistically significant condition-related differences ($p < .05$; Figure 4C). On the basis of the contour lines observed in the topographical map, we explored the interaction patterns of C5 and P8 separately. For C5, the main effect of Current-Trial Congruency was not significant, $F(1, 29) = 2.05, p = .162$. However, a significant interaction between Previous-Trial Congruency and Current-Trial Congruency was found, $F(1, 29) = 8.46, p = .006, MSE = 11.87, \eta_p^2 = .225$. The difference between cI and iI was not significant, $F(1, 29) < 1$. However, a significant cluster was observed across conditions (cluster-corrected, $p < .05$), starting approximately 220 msec after stimulus presentation and continuing until 720 msec. Although a significant cluster was identified at C5, the interaction observed did not follow the typical pattern of the CSE (Figure 1). For P8, the main effect of Current-Trial Congruency was not significant, $F(1, 29) < 1$. A significant interaction between Previous-Trial Congruency and Current-Trial Congruency was found, $F(1, 29) = 4.7, p = .038, MSE = 14.02, \eta_p^2 = .139$. The difference between cI and iI was significant, $F(1, 29) = 6.96, p = .013, MSE = 16.19, \eta_p^2 = .193$. However, no clusters were observed at P8, and the interaction at this electrode also did not follow the typical CSE pattern (Figure 1).

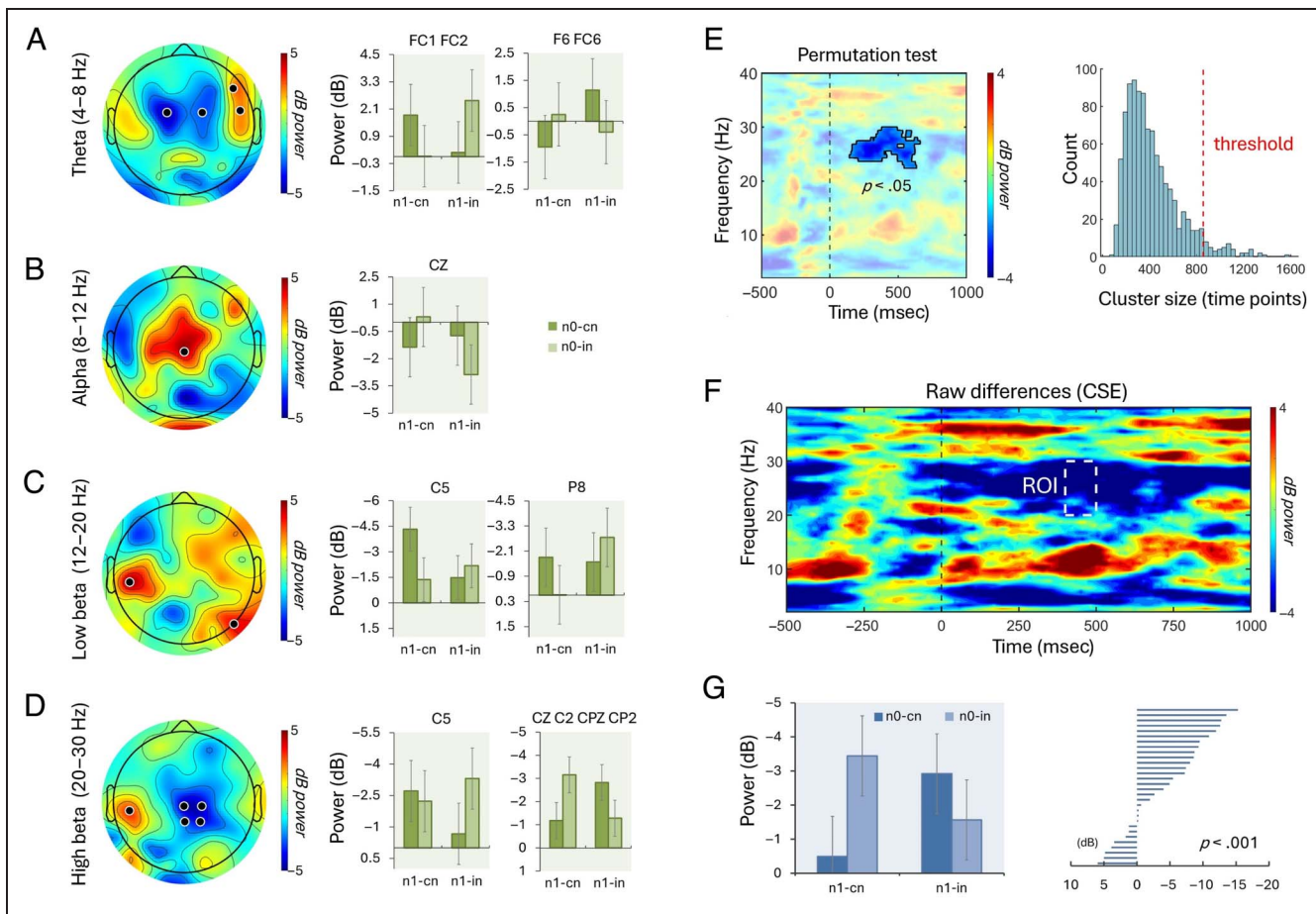


Figure 4. Time–frequency power results. Topographies show condition differences across different frequency bands: (A) theta (4–8 Hz), (B) alpha (8–12 Hz), (C) low beta (12–20 Hz), and (D) high beta (20–30 Hz). Black dots indicate electrodes with significant condition-related differences ($p < .05$). Electrodes were grouped based on topographical contours for further analysis. The bar graphs to the right display averaged data for four conditions (cC, cI, iC, and iI) in channels with significant effects from 400 to 500 msec. To enhance the intuitive interpretation of the CSE pattern, the y axis was inverted in graphs where the power values for all conditions (cC, cI, iC, iI) were negative. In the high beta band, averaged data from electrodes Cz, C2, CPz, and CP2 show a typical CSE pattern, indicating conflict resolution. Cz was ultimately selected for further analysis based on these results and previous studies. (E) The cluster-based permutation test for Cz reveals a significant cluster on the z map, with cluster size distribution shown alongside. (F) ROIs are highlighted within the raw condition differences (i.e., CSE). (G) Averaged power for each condition (cC, cI, iC, and iI) from the ROI (left) and individual CSE results (right).

High Beta (20–30 Hz)

Electrodes C5, Cz, C2, CPz, and CP2 exhibited statistically significant condition-related differences ($p < .05$; Figure 4D). On the basis of the contour lines observed in the topographical map, we analyzed the interaction patterns of C5 separately from the group of Cz, C2, CPz, and CP2. For C5, the main effect of Current-Trial Congruency was not significant, $F(1, 29) = 2.88$, $p = .100$. However, a significant interaction between Previous-Trial Congruency and Current-Trial Congruency was found, $F(1, 29) = 4.8$, $p = .036$, $MSE = 15.28$, $\eta_p^2 = .142$. The difference between cI and iI was not significant, $F(1, 29) = 1.2$, $p = .28$. No significant clusters were observed at C5, and the interaction did not follow the typical pattern of the CSE (Figure 1).

For the group of Cz, C2, CPz, and CP2, the main effect of Current-Trial Congruency was also not significant, $F(1, 29) < 1$. However, a significant interaction between Previous-Trial Congruency and Current-Trial Congruency was observed, $F(1, 29) = 21.38$, $p < .001$, $MSE = 4.32$, $\eta_p^2 = .424$. The difference between cI and iI was significant, $F(1, 29) = 6.88$, $p = .013$, $MSE = 7.63$, $\eta_p^2 = .191$. Importantly, the interaction pattern closely followed the typical CSE pattern (Figure 4D and Figure 1). In addition, a significant cluster was observed across conditions (cluster-corrected, $p < .05$), beginning approximately 170 msec after stimulus presentation and continuing until 580 msec. Given that Cz is the electrode most commonly associated with top-down cognitive control in previous literature, we selected Cz for further time–frequency analysis.

Time–Frequency Analysis at Cz

In the cluster-based analysis, a significant reduction of power was observed in the high beta band (20–30 Hz) across conditions (cluster-corrected, $p < .05$; Figure 4E). This reduction started approximately 150 msec after stimulus presentation and continued until 640 msec. No other clusters were found in other time and frequency domains. For the ROI analysis, time–frequency windows were selected from 400 to 500 msec at 20–30 Hz. The main effect of previous-trial congruency was not significant, $F(1, 29) < 1$. The main effect of current-trial congruency was not significant, $F(1, 29) = 1.17, p = .288$. However, a significant interaction was obtained between previous-trial congruency and current-trial congruency, $F(1, 29) = 14.06, p < .001, MSE = 9.85, \eta_p^2 = .326$, indicating a significant CSE was observed in high beta oscillations (Figure 4F and G). Moreover, a significant difference was found between the cI and iI conditions, $F(1, 29) = 5.34, p = .028, MSE = 9.88, \eta_p^2 = .155$. These results demonstrate that the decoding findings were validated through global time–frequency analysis.

Brain–Behavior Correlation

In exploratory analyses, we examined whether the EEG measure (i.e., decoding and the pattern in time–frequency analyses) might be correlated with the behavioral measure of the CSE. For the decoding analysis, we focused on location decoding within the 400- to 500-msec time window in the high beta frequency range (20–30 Hz), where the difference in classification performance (AUC) between previous congruent and incongruent trials was most pronounced. Within this time window, we calculated each participant’s mean AUC for both congruent and incongruent conditions and then computed the difference between these two values. For the time–frequency analysis, we calculated each participant’s mean ROI values for the cC, cI, iC, and iI conditions within the same frequency and time window used for the decoding analysis. On the basis of the differences in ROI values across conditions, we then computed the CSE. For behavioral outcomes, we calculated the magnitude of the CSE for TT, IT, and MT. Finally, Pearson correlation analyses were conducted by comparing individual differences in IT, MT, and TT with both the decoding differences and the power differences obtained from the time–frequency analysis. Across all analyses, no significant correlations were observed (all p values $> .05$). We speculate that the lack of correlation might be driven, in part, by the smaller sample size ($n = 30$) compared with the proposed sample size for detecting a medium effect size ($n = 84$ for correlation coefficient $r = .3$; Brysbaert, 2019). Future research with a larger sample is necessary to examine the relationship between EEG and behavioral measures of the CSE.

DISCUSSION

In this study, we investigated how cognitive control resolves Simon conflicts and selectively processes information following incongruent trials. We decoded human scalp EEG data during Simon tasks to determine if brain representations of goal and distractor information change based on previous-trial congruency. In behavior analysis, we found a significant CSE in RTs, indicating that top-down cognitive control was heightened after incongruent trials. In addition, a CSE was observed in MT, suggesting that conflict resolution is more likely to occur at a later stage of information processing. Presumably, this occurs during the period from the release of the home key (averaging approximately 384 msec; Table 1) to the moment the actual response is made (averaging approximately 508 msec; Table 1). Decoding analysis demonstrated that there was no difference in location decoding between the two conditions (n1-cn and n1-in) during the first time window (0–300 msec), indicating that the neural representations of location were similar in both conditions. However, in location decoding during the response phase (400–520 msec), the decoding accuracy of the task-irrelevant location significantly decreased after incongruent trials compared with congruent trials, particularly in the high beta frequency band (20–30 Hz), suggesting a suppression effect on task-irrelevant information following conflict. Conversely, no such difference was observed in the decoding of task-relevant color information. Time–frequency analysis revealed a significant CSE in the high beta frequency band (20–30 Hz), further confirming that top-down cognitive control for Simon conflict resolution is associated with high beta oscillations. These findings strongly support the idea that conflict resolution in Simon tasks is closely linked to the inhibition of task-irrelevant information processing and occurs during the movement execution stage.

The CSE is a hypothesized marker of top-down cognitive control, which has been served as an important research tool for investigating the operation of the cognitive control. By testing whether the CSE transfers across different task conditions (e.g., conflict type, task sets, distractor type), researchers specify the scope of cognitive control and infer the mechanism involved in cognitive control processes (Braem, Abrahamse, Duthoo, & Notebaert, 2014). Two different types of mechanisms have been proposed: (a) biasing stimulus processing and (b) biasing response processing (Soutschek, Müller, & Schubert, 2013; Egner, Delano, & Hirsch, 2007). Egner and colleagues (2007) suggested that these two types of conflict resolution processes depend on the source of conflict. In their combined Stroop–Simon color naming task, participants were instructed to respond to the ink color of a word presented to the left or right of fixation, while ignoring both the word’s meaning (Stroop conflict) and its location (Simon conflict). Notably, significant CSEs were observed within the same conflict type but not across different conflicts.

The author suggested that the absence of the CSE between Stroop and Simon conflicts is due to independent control processes resolving each type of conflict. Specifically, Stroop conflict is resolved through early stimulus-biasing, enhancing the processing of task-relevant information, whereas Simon conflict is resolved through late response-biasing, involving the suppression of the task-irrelevant information processing. This distinction was further supported by fMRI findings, which showed that the resolution of Stroop conflict was associated with the recruitment of superior parietal cortex, whereas the resolution of the Simon conflict was associated with the recruitment of ventral premotor cortex.

However, inconsistent with the source of conflict account, Akçay and Hazeltine (2008) found that the CSE was transferred across tasks only when the stimulus and response alternatives for two Simon tasks displayed on the same hemisphere, but not when one Simon task was presented in the left and the other presented in the right hemisphere. The authors suggested that the degree to which participants perceive the Simon tasks as a single or different tasks determines whether the conflict is resolved by the same or different control processes. It has been suggested that this task representation or task-sets formed based on salient perceptual features, such as task-relevant features (Braem et al., 2014) or the sensory modality of task stimuli (Yang et al., 2017; Hazeltine, Lightman, Schwarb, & Schumacher, 2011), and the predictability of the task (Grant et al., 2020). Therefore, if two tasks are separated in terms of a salient feature, participants use this salient feature to divide a complex task into two or more simpler tasks, or different task-sets to aid task performance (Grant & Weissman, 2023). This emerging view of the CSE is known as the episodic retrieval account (Grant & Weissman, 2023; Grant et al., 2020; Dignath, Johannsen, Hommel, & Kiesel, 2019; Weissman, Hawks, & Egner, 2016). The account suggests that participants form episodic memories of the task set, which includes information about stimuli, responses, context-defining features, and the relationships governed by task rules. When any of these contextual features are repeated on subsequent trials, they trigger the retrieval of the previous trial's memory, leading control processes to adopt the same settings. This results in a reduced congruency effect following incongruent trials compared with congruent trials.

However, Lee and Cho (2023) found that the CSE transferred across Simon tasks that were highly distinguished by sensory modality, task predictability, and task-relevant dimension, all of which are essential for differentiating a task set. This indicates that differences in these salient features do not determine the transfer of the CSE between Simon tasks. Because the only components shared between the tasks were the task-irrelevant dimension and response mode, which are critical for response

suppression (Lim & Cho, 2021b; Kim, Lee, & Cho, 2015; Lee & Cho, 2013; Stürmer et al., 2002), the authors concluded that conflict resolution in Simon tasks primarily occurs at the automatic route between the task-irrelevant dimension and response mode. This conclusion was further supported by Lee and Cho (2024), in which no transfer of the CSE was found when the task-irrelevant spatial dimensions differed across tasks (e.g., spatial word meaning versus spatial location), indicating that cognitive control mechanisms in the Simon task operate on task-irrelevant dimensions.

Consistent with these studies, our decoding results revealed that decoding accuracy for task-irrelevant information changed as a function of previous congruency, whereas no such modulation was observed for task-relevant information, indicating that conflict resolution in the Simon task primarily occurs at the task-irrelevant dimension. More importantly, decoding accuracy for task-irrelevant information was significantly reduced after incongruent trials compared with after congruent trials. This suggests that conflict resolution operated by suppressing the task-irrelevant information processing after experiencing conflict. Thus, building on the previous study that demonstrated the scope of conflict resolution in the Simon task (Lee & Cho, 2023), our study is the first to provide direct evidence of how Simon conflicts are resolved through inhibition, which offers valuable insights into the mechanisms underlying top-down cognitive control.

Neural oscillations, often referred to as brain rhythms, are periodic patterns of electrical activity in the brain that arise from the synchronized activity of neurons (Fries, 2005). These oscillations are categorized into different frequency bands, which are linked to distinct cognitive and behavioral functions (Buzsáki, 2006). Among these brain rhythms, oscillations in the beta frequency range (13–30 Hz) are particularly associated with sensorimotor processing (Schmidt et al., 2019; Spitzer & Haegens, 2017; Pavlidou et al., 2014; Engel & Fries, 2010; Baker, 2007; Pfurtscheller, Stancak Jr, & Neuper, 1996). During movement preparation and execution, beta power decreases, while an increase in beta power in sensorimotor areas reflects active suppression of the motor system. For example, modulations of sensorimotor beta power have been observed during the observation of correct versus incorrect movements, with decreased beta power for incorrect movements, suggesting that sensorimotor beta oscillations might be involved in evaluating observed movement (Koelewijn, van Schie, Bekkering, Oostenveld, & Jensen, 2008). Moreover, increased beta power at frontal scalp EEG electrodes is also associated with movement stopping (e.g., Swann et al., 2009, 2012). Using intracranial EEG, studies have reported increases in beta band activity in the right inferior frontal gyrus during successful stop trials compared with unsuccessful trials. These findings suggest that beta power may serve as a critical indicator of motor suppression.

Beyond its established role as a sensorimotor rhythm, beta oscillations have been implicated in a wide range of cognitive functions, primarily associated with top-down controlled processing (Fries, 2015; Engel & Fries, 2010; Wang, 2010; Buschman & Miller, 2007). According to the status-quo theory proposed by Engel and Fries (2010), beta oscillations are involved in maintaining a motor and/or cognitive state. Specifically, the theory proposed that the level of beta band activity remains constant when there is no change in the cognitive or perceptual set, increases when the current cognitive set has to be maintained, and decreases when the current setting is disrupted by a novel or unexpected event. Evidence supporting this theory comes from Buschman and Miller (2007), demonstrating a strong link between top-down processing and beta-band activity. In their study, monkeys were trained to find a target among distractors using either a pop-out mode (where the target is easily distinguishable from the distractors) or a serial search mode (where the target shares some features with distractors and is thus less distinguishable). They found that beta-band coherence between frontal and parietal regions was prevalent during serial searches, which required strong top-down processing. In contrast, gamma-band coupling was more significant during pop-out searches, which relied on bottom-up saliency of the target. These results suggest that beta oscillations are involved in endogenous top-down control, whereas gamma oscillations convey exogenous bottom-up signals. Consistent with this finding, numerous studies have also linked beta oscillations to top-down cognitive control (Cunillera et al., 2012; Axmacher, Schmitz, Wagner, Elger, & Fell, 2008; Deiber et al., 2007; Gladwin, Lindsen, & de Jong, 2006).

Our results further verify the strong association between beta oscillations and top-down cognitive control, specifically in terms of inhibition. The time-frequency analysis (Figure 4G, left) revealed that when the current trial was incongruent (i.e., n0-in), high beta power significantly increased when the previous trial was incongruent (i.e., n1-in) compared with when it was congruent (i.e., n1-cn). This finding suggests that top-down control is enhanced following conflict experience. In addition, location decoding in high beta band was significantly decreased following incongruent trials compared with following congruent trials. Thus, by demonstrating top-down cognitive control in the CSE within the beta-frequency band in the context of a bottom-up confound-minimized paradigm, our findings provide clear evidence of this association. Importantly, because these effects were observed in the Simon task, our study raises the possibility that beta oscillations are specifically related to inhibition. Together, we interpret beta frequency in our task as the electrophysiological signature of the conflict resolution process, specifically reflecting response suppression activated by inhibitory control to prevent strong, unwanted habitual behaviors.

The observed differences in the location decoding between congruent and incongruent trials in high beta band frequency may indicate that attention was more evenly distributed between task-relevant and task-irrelevant features following congruent trials and that more attention was allocated to task-relevant information following incongruent trials. However, our findings are not consistent with this prediction because the color decoding following incongruent trials was not better than following congruent trials. In addition, the location decoding was initially (i.e., 0–300 msec) comparable between the two types of trials, suggesting no initial differences in attentional allocation. Instead, the temporal dynamics of decoding indicate that attention to location information was maintained with some fluctuation after congruent trials but gradually diminished after incongruent trials. These results suggest that the cognitive control mechanism inhibited the processing of task-irrelevant information, consistent with the previous findings in conflict resolution in the Simon task (Lee & Cho, 2013, 2023, 2024; Kim et al., 2015; Soutschek et al., 2013; Egner et al., 2007; Stürmer et al., 2002). However, we note that there is evidence that cognitive control enhances the processing of task-relevant information in the case of the Stroop effect (Purmann & Pollmann, 2015; Notebaert & Verguts, 2008; Egner et al., 2007; Egner & Hirsch, 2005). Therefore, we do not completely rule out the enhancement of task-relevant information following cognitive conflict. Instead, we conclude that the primary cognitive control mechanism for resolving Simon-type conflict relies more on distractor inhibition.

The absence of theta oscillation in the Simon task is noteworthy, as it contrasts with the extensive literature that emphasizes the importance of theta band activity in conflict resolution. We propose two potential explanations for this finding, primarily focusing on differences in experimental paradigms. Our confound-minimized design, in which no stimulus or response attributes were repeated across trials, may have emphasized inhibition more than other cognitive control functions, such as working memory and cognitive flexibility. Because inhibition is closely tied to sensorimotor processing, beta activity became more prominent in our study. Another possible explanation is the response method used in our task, which is more refined than the traditional keypress method. Previous research has shown that tasks responded with mouse-tracking-elicited beta oscillations (Palmer, Auksztulewicz, Ondobaka, & Kilner, 2019), which is similar to the present response method that divides responses into IT, MT, and TT. Thus, using an aimed movement method, which is relatively more complex than the keypress method, may have either consumed attentional resources toward the goal or unintentionally enhanced inhibitory processing.

Although our aimed-movement approach, which included maintaining pressure on the home key, might have contributed to our results by depleting cognitive

resources due to the effort required to resist the impulse to release the home key, this alone does not fully explain our findings. If this were the case, we would expect a general increase in RTs or an overall weakening of the Simon effect across both conditions (n1-cn and n1-in). However, we found that the magnitude of the Simon effect was modulated by the congruency of the previous trial, rather than by a general performance decrement independent of the previous trial's congruency, which cannot be fully explained by general resource depletion alone. Moreover, previous studies replicated the CSE using a more cognitively demanding method (i.e., aimed-movements with mouse tracking) than simple keypresses (Ye & Damian, 2023), indicating that tasks with higher cognitive demand do not necessarily undermine the observation of CSE. Similarly, if home key maintenance indeed strengthened inhibition, we should have observed an overall enhancement of inhibitory effects. Yet, our study found a reduction in the Simon effect following incongruent trials only. Lastly, our findings (i.e., a reduced Simon effect following incongruent trials) are consistent with findings from previous studies that used a more typical RT measure (Kim et al., 2015; Lee & Cho, 2013; Soutschek et al., 2013; Egner et al., 2007). On the basis of these points, we conclude that home key maintenance alone cannot fully account for our key findings.

In conclusion, the present study demonstrates that the CSE in top-down cognitive control inherently involves inhibition, with its foundation resting on the suppression of distractor processing. This modulation is reflected in the beta activity, which is recognized for its association with top-down cognitive control and motor inhibition. It is important to note that the present study does not claim to have completely ruled out other cognitive control processes that also contribute to sequential modulation in the Simon task. For instance, working memory is also an important component that influences Simon sequential modulation, depending on specific attributes of a given paradigm. Nevertheless, our findings highlight the important role of inhibition in the CSE, suggesting that the suppression of distractor representation is a key mechanism underlying Simon conflict resolution.

Corresponding author: Yang Seok Cho, School of Psychology, Korea University, Seoul, 02841, South Korea, e-mail: yscho_psych@korea.ac.kr.

Data Availability Statement

Data are available upon request from the authors.

Author Contributions

Yoon Seo Lee: Conceptualization; Data curation; Formal analysis; Investigation; Methodology; Writing—Original

draft; Writing—Review & editing. Gi-Yeul Bae: Conceptualization; Methodology; Writing—Review & editing. Yang Seok Cho: Conceptualization; Funding acquisition; Project administration; Writing—Review & editing.

Funding Information

This research was supported by a Korean Research Foundation grant funded by the Korean Government (NRF-2020R1A2C2012033).

Diversity in Citation Practices

Retrospective analysis of the citations in every article published in this journal from 2010 to 2021 reveals a persistent pattern of gender imbalance: Although the proportions of authorship teams (categorized by estimated gender identification of first author/last author) publishing in the *Journal of Cognitive Neuroscience* (*JoCN*) during this period were M(an)/M = .407, W(oman)/M = .32, M/W = .115, and W/W = .159, the comparable proportions for the articles that these authorship teams cited were M/M = .549, W/M = .257, M/W = .109, and W/W = .085 (Postle and Fulvio, *JoCN*, 34:1, pp. 1–3). Consequently, *JoCN* encourages all authors to consider gender balance explicitly when selecting which articles to cite and gives them the opportunity to report their article's gender citation balance.

REFERENCES

- Akçay, Ç., & Hazeltine, E. (2008). Conflict adaptation depends on task structure. *Journal of Experimental Psychology: Human Perception and Performance*, 34, 958–973. <https://doi.org/10.1037/0096-1523.34.4.958>, PubMed: 18665738
- Arnau, S., Brümmer, T., Liegel, N., & Wascher, E. (2021). Inverse effects of time-on-task in task-related and task-unrelated theta activity. *Psychophysiology*, 58, e13805. <https://doi.org/10.1111/psyp.13805>, PubMed: 33682172
- Axmacher, N., Schmitz, D. P., Wagner, T., Elger, C. E., & Fell, J. (2008). Interactions between medial temporal lobe, prefrontal cortex, and inferior temporal regions during visual working memory: A combined intracranial EEG and functional magnetic resonance imaging study. *Journal of Neuroscience*, 28, 7304–7312. <https://doi.org/10.1523/JNEUROSCI.1778-08.2008>, PubMed: 18632934
- Bae, G.-Y. (2020). The time course of face representations during perception and working memory maintenance. *Cerebral Cortex*, 2, tga093. <https://doi.org/10.1093/texcom/tga093>, PubMed: 34296148
- Bae, G.-Y., & Chen, K.-W. (2024). EEG decoding reveals task-dependent recoding of sensory information in working memory. *Neuroimage*, 297, 120710. <https://doi.org/10.1016/j.neuroimage.2024.120710>, PubMed: 38942100
- Bae, G.-Y., & Luck, S. J. (2018). Dissociable decoding of spatial attention and working memory from EEG oscillations and sustained potentials. *Journal of Neuroscience*, 38, 409–422. <https://doi.org/10.1523/JNEUROSCI.2860-17.2017>, PubMed: 29167407

- Bae, G.-Y., & Luck, S. J. (2019). Reactivation of previous experiences in a working memory task. *Psychological Science*, *30*, 587–595. <https://doi.org/10.1177/0956797619830398>, PubMed: 30817224
- Baker, S. N. (2007). Oscillatory interactions between sensorimotor cortex and the periphery. *Current Opinion in Neurobiology*, *17*, 649–655. <https://doi.org/10.1016/j.conb.2008.01.007>, PubMed: 18339546
- Ball, R., Shu, C., Xi, P., Rioux, M., Luximon, Y., & Molendbroek, J. (2010). A comparison between Chinese and Caucasian head shapes. *Applied Ergonomics*, *41*, 832–839. <https://doi.org/10.1016/j.apergo.2010.02.002>, PubMed: 20227060
- Beatty, P. J., Buzzell, G. A., Roberts, D. M., Voloshyna, Y., & McDonald, C. G. (2021). Subthreshold error corrections predict adaptive post-error compensations. *Psychophysiology*, *58*, e13803. <https://doi.org/10.1111/psyp.13803>, PubMed: 33709470
- Botvinick, M., Nystrom, L. E., Fissell, K., Carter, C. S., & Cohen, J. D. (1999). Conflict monitoring versus selection-for-action in anterior cingulate cortex. *Nature*, *402*, 179–181. <https://doi.org/10.1038/46035>, PubMed: 10647008
- Botvinick, M. M., Braver, T. S., Barch, D. M., Carter, C. S., & Cohen, J. D. (2001). Conflict monitoring and cognitive control. *Psychological Review*, *108*, 624–652. <https://doi.org/10.1037/0033-295X.108.3.624>, PubMed: 11488380
- Braem, S., Abrahamse, E. L., Duthoo, W., & Notebaert, W. (2014). What determines the specificity of conflict adaptation? A review, critical analysis, and proposed synthesis. *Frontiers in Psychology*, *5*, 1134. <https://doi.org/10.3389/fpsyg.2014.01134>, PubMed: 25339930
- Brysbaert, M. (2019). How many participants do we have to include in properly powered experiments? A tutorial of power analysis with reference tables. *Journal of Cognition*, *2*, 16. <https://doi.org/10.5334/joc.72>, PubMed: 31517234
- Buetti, S., & Kerzel, D. (2008). Time course of the Simon effect in pointing movements for horizontal, vertical, and acoustic stimuli: Evidence for a common mechanism. *Acta Psychologica*, *129*, 420–428. <https://doi.org/10.1016/j.actpsy.2008.09.007>, PubMed: 18930170
- Buetti, S., & Kerzel, D. (2009). Conflicts during response selection affect response programming: Reactions toward the source of stimulation. *Journal of Experimental Psychology: Human Perception and Performance*, *35*, 816–834. <https://doi.org/10.1037/a0011092>, PubMed: 19485694
- Buschman, T. J., & Miller, E. K. (2007). Top-down versus bottom-up control of attention in the prefrontal and posterior parietal cortices. *Science*, *315*, 1860–1862. <https://doi.org/10.1126/science.1138071>, PubMed: 17395832
- Buzsáki, G. (2006). *Rhythms of the brain*. Oxford University Press. <https://doi.org/10.1093/acprof:oso/9780195301069.001.0001>
- Calderon, C. B., Gevers, W., & Verguts, T. (2018). The unfolding action model of initiation times, movement times, and movement paths. *Psychological Review*, *125*, 785–805. <https://doi.org/10.1037/rev0000110>, PubMed: 30160511
- Cao, Y., Cao, X., Yue, Z., & Wang, L. (2017). Temporal and spectral dynamics underlying cognitive control modulated by task-irrelevant stimulus-response learning. *Cognitive, Affective, & Behavioral Neuroscience*, *17*, 158–173. <https://doi.org/10.3758/s13415-016-0469-5>, PubMed: 27752940
- Chen, S., & Melara, R. D. (2009). Sequential effects in the Simon task: Conflict adaptation or feature integration? *Brain Research*, *1297*, 89–100. <https://doi.org/10.1016/j.brainres.2009.08.003>, PubMed: 19666010
- Chinn, L. K., Pauker, C. S., & Golob, E. J. (2018). Cognitive control and midline theta adjust across multiple timescales. *Neuropsychologia*, *111*, 216–228. <https://doi.org/10.1016/j.neuropsychologia.2018.01.031>, PubMed: 29410123
- Clayson, P. E., & Larson, M. J. (2011). Effects of repetition priming on electrophysiological and behavioral indices of conflict adaptation and cognitive control. *Psychophysiology*, *48*, 1621–1630. <https://doi.org/10.1111/j.1469-8986.2011.01265.x>, PubMed: 21806636
- Cohen, M. X. (2014). *Analyzing neural time series data: Theory and practice*. Cambridge, MA: MIT Press. <https://doi.org/10.7551/mitpress/9609.001.0001>
- Cohen, M. X., & Donner, T. H. (2013). Midfrontal conflict-related theta-band power reflects neural oscillations that predict behavior. *Journal of Neurophysiology*, *110*, 2752–2763. <https://doi.org/10.1152/jn.00479.2013>, PubMed: 24068756
- Cohen, M. X., & Ridderinkhof, K. R. (2013). EEG source reconstruction reveals frontal-parietal dynamics of spatial conflict processing. *PLoS One*, *8*, e57293. <https://doi.org/10.1371/journal.pone.0057293>, PubMed: 23451201
- Cunillera, T., Fuentemilla, L., Periañez, J., Marco-Pallarès, J., Krämer, U. M., Càmara, E., et al. (2012). Brain oscillatory activity associated with task switching and feedback processing. *Cognitive, Affective, & Behavioral Neuroscience*, *12*, 16–33. <https://doi.org/10.3758/s13415-011-0075-5>, PubMed: 22160843
- De Jong, R., Liang, C.-C., & Lauber, E. (1994). Conditional and unconditional automaticity: A dual-process model of effects of spatial stimulus-response correspondence. *Journal of Experimental Psychology: Human Perception and Performance*, *20*, 731–750. <https://doi.org/10.1037/0096-1523.20.4.731>, PubMed: 8083631
- Deiber, M.-P., Missonnier, P., Bertrand, O., Gold, G., Fazio-Costa, L., Ibañez, V., et al. (2007). Distinction between perceptual and attentional processing in working memory tasks: A study of phase-locked and induced oscillatory brain dynamics. *Journal of Cognitive Neuroscience*, *19*, 158–172. <https://doi.org/10.1162/jocn.2007.19.1.158>, PubMed: 17214572
- Delorme, A., & Makeig, S. (2004). EEGLAB: An open source toolbox for analysis of single-trial EEG dynamics including independent component analysis. *Journal of Neuroscience Methods*, *134*, 9–21. <https://doi.org/10.1016/j.jneumeth.2003.10.009>, PubMed: 15102499
- de Vries, I. E. J., Marinato, G., & Baldauf, D. (2021). Decoding object-based auditory attention from source-reconstructed MEG alpha oscillations. *Journal of Neuroscience*, *41*, 8603–8617. <https://doi.org/10.1523/JNEUROSCI.0583-21.2021>, PubMed: 34429378
- de Vries, I. E. J., Savran, E., van Driel, J., & Olivers, C. N. (2019). Oscillatory mechanisms of preparing for visual distraction. *Journal of Cognitive Neuroscience*, *31*, 1873–1894. https://doi.org/10.1162/jocn_a_01460, PubMed: 31418334
- Diamond, A. (2013). Executive functions. *Annual Review of Psychology*, *64*, 135–168. <https://doi.org/10.1146/annurev-psych-113011-143750>, PubMed: 23020641
- Dignath, D., Johannsen, L., Hommel, B., & Kiesel, A. (2019). Reconciling cognitive-control and episodic-retrieval accounts of sequential conflict modulation: Binding of control-states into event-files. *Journal of Experimental Psychology: Human Perception and Performance*, *45*, 1265–1270. <https://doi.org/10.1037/xhp0000673>, PubMed: 31380673
- Drisdelle, B. L., Aubin, S., & Jolicœur, P. (2017). Dealing with ocular artifacts on lateralized ERPs in studies of visual-spatial attention and memory: ICA correction versus epoch rejection. *Psychophysiology*, *54*, 83–99. <https://doi.org/10.1111/psyp.12675>, PubMed: 28000252
- Dubois, J., & Adolphs, R. (2016). Building a science of individual differences from fMRI. *Trends in Cognitive Sciences*, *20*, 425–443. <https://doi.org/10.1016/j.tics.2016.03.014>, PubMed: 27138646

- Duprez, J., Gulbinaite, R., & Cohen, M. X. (2020). Midfrontal theta phase coordinates behaviorally relevant brain computations during cognitive control. *Neuroimage*, 207, 116340. <https://doi.org/10.1016/j.neuroimage.2019.116340>, PubMed: 31707192
- Duprez, J., Houvenaghel, J.-F., Dondaine, T., Péron, J., Haegelen, C., Drapier, S., et al. (2019). Subthalamic nucleus local field potentials recordings reveal subtle effects of promised reward during conflict resolution in Parkinson's disease. *Neuroimage*, 197, 232–242. <https://doi.org/10.1016/j.neuroimage.2019.04.071>, PubMed: 31051290
- Eder, A. B., Leuthold, H., Rothermund, K., & Schweinberger, S. R. (2012). Automatic response activation in sequential affective priming: An ERP study. *Social Cognitive and Affective Neuroscience*, 7, 436–445. <https://doi.org/10.1093/scan/nsr033>, PubMed: 21642351
- Egner, T., Delano, M., & Hirsch, J. (2007). Separate conflict-specific cognitive control mechanisms in the human brain. *Neuroimage*, 35, 940–948. <https://doi.org/10.1016/j.neuroimage.2006.11.061>, PubMed: 17276088
- Egner, T., & Hirsch, J. (2005). Cognitive control mechanisms resolve conflict through cortical amplification of task-relevant information. *Nature Neuroscience*, 8, 1784–1790. <https://doi.org/10.1038/nn1594>, PubMed: 16286928
- Engel, A. K., & Fries, P. (2010). Beta-band oscillations—Signalling the status quo? *Current Opinion in Neurobiology*, 20, 156–165. <https://doi.org/10.1016/j.conb.2010.02.015>, PubMed: 20359884
- Erlhagen, W., & Schöner, G. (2002). Dynamic field theory of movement preparation. *Psychological Review*, 109, 545–572. <https://doi.org/10.1037/0033-295x.109.3.545>, PubMed: 12088245
- Fahrenfort, J. J., van Driel, J., van Gaal, S., & Olivers, C. N. L. (2018). From ERPs to MVPA using the Amsterdam Decoding and Modeling toolbox (ADAM). *Frontiers in Neuroscience*, 12, 368. <https://doi.org/10.3389/fnins.2018.00368>, PubMed: 30018529
- Fan, J., Byrne, J., Worden, M. S., Guise, K. G., McCandliss, B. D., Fossella, J., et al. (2007). The relation of brain oscillations to attentional networks. *Journal of Neuroscience*, 27, 6197–6206. <https://doi.org/10.1523/JNEUROSCI.1833-07.2007>, PubMed: 17553991
- Faul, F., Erdfelder, E., Buchner, A., & Lang, A. G. (2009). Statistical power analyses using G*Power 3.1: Tests for correlation and regression analyses. *Behavior Research Methods*, 41, 1149–1160. <https://doi.org/10.3758/brm.41.4.1149>, PubMed: 19897823
- Foster, J. J., & Awh, E. (2019). The role of alpha oscillations in spatial attention: Limited evidence for a suppression account. *Current Opinion in Psychology*, 29, 34–40. <https://doi.org/10.1016/j.copsyc.2018.11.001>, PubMed: 30472541
- Frackowiak, R. S. J., Friston, K. J., Frith, C. D., Dolan, R. J., Price, C. J., Zeki, S., et al. (2004). *Human brain function* (2nd ed.). Elsevier Academic Press. <https://doi.org/10.1016/B978-0-12-264841-0.X5000-8>
- Fries, P. (2005). A mechanism for cognitive dynamics: Neuronal communication through neuronal coherence. *Trends in Cognitive Sciences*, 9, 474–480. <https://doi.org/10.1016/j.tics.2005.08.011>, PubMed: 16150631
- Fries, P. (2015). Rhythms for cognition: Communication through coherence. *Neuron*, 88, 220–235. <https://doi.org/10.1016/j.neuron.2015.09.034>, PubMed: 26447583
- Fröhholz, S., Godde, B., Finke, M., & Herrmann, M. (2011). Spatio-temporal brain dynamics in a combined stimulus-stimulus and stimulus-response conflict task. *Neuroimage*, 54, 622–634. <https://doi.org/10.1016/j.neuroimage.2010.07.071>, PubMed: 20691791
- Gladwin, T. E., Lindsen, J. P., & de Jong, R. (2006). Pre-stimulus EEG effects related to response speed, task switching and upcoming response hand. *Biological Psychology*, 72, 15–34. <https://doi.org/10.1016/j.biopsych.2005.05.005>, PubMed: 16169147
- Grant, L. D., Cookson, S. L., & Weissman, D. H. (2020). Task sets serve as boundaries for the congruency sequence effect. *Journal of Experimental Psychology: Human Perception and Performance*, 46, 798–812. <https://doi.org/10.1037/xhp0000750>, PubMed: 32324028
- Grant, L. D., & Weissman, D. H. (2023). The binary structure of event files generalizes to abstract features: A nonhierarchical explanation of task set boundaries for the congruency sequence effect. *Journal of Experimental Psychology: Learning, Memory, and Cognition*, 49, 1033–1050. <https://doi.org/10.1037/xlm0001148>, PubMed: 35951436
- Gratton, G., Coles, M. G. H., & Donchin, E. (1992). Optimizing the use of information: Strategic control of activation of responses. *Journal of Experimental Psychology: General*, 121, 480–506. <https://doi.org/10.1037/0096-3445.121.4.480>, PubMed: 1431740
- Gulbinaite, R., van Rijn, H., & Cohen, M. X. (2014). Fronto-parietal network oscillations reveal relationship between working memory capacity and cognitive control. *Frontiers in Human Neuroscience*, 8, 761. <https://doi.org/10.3389/fnhum.2014.00761>, PubMed: 25324759
- Hazeltine, E., Lightman, E., Schwab, H., & Schumacher, E. H. (2011). The boundaries of sequential modulations: Evidence for set-level control. *Journal of Experimental Psychology: Human Perception and Performance*, 37, 1898–1914. <https://doi.org/10.1037/a0024662>, PubMed: 21767054
- Hommel, B. (2009). Action control according to TEC (theory of event coding). *Psychological Research*, 73, 512–526. <https://doi.org/10.1007/s00426-009-0234-2>, PubMed: 19337749
- Hommel, B., Proctor, R. W., & Vu, K.-P. L. (2004). A feature-integration account of sequential effects in the Simon task. *Psychological Research*, 68, 1–17. <https://doi.org/10.1007/s00426-003-0132-y>, PubMed: 14752663
- Hoppe, K., Küper, K., & Wascher, E. (2017). Sequential modulations in a combined horizontal and vertical Simon task: Is there ERP evidence for feature integration effects? *Frontiers in Psychology*, 8, 1094. <https://doi.org/10.3389/fpsyg.2017.01094>, PubMed: 28713305
- Ignatiadis, K., Barumerli, R., Tóth, B., & Baumgartner, R. (2022). Effects of individualized brain anatomies and EEG electrode positions on inferred activity of the primary auditory cortex. *Frontiers in Neuroinformatics*, 16, 970372. <https://doi.org/10.3389/fninf.2022.970372>, PubMed: 36313125
- Jansen, M., White, T. P., Mullinger, K. J., Liddle, E. B., Gowland, P. A., Francis, S. T., et al. (2012). Motion-related artefacts in EEG predict neuronally plausible patterns of activation in fMRI data. *Neuroimage*, 59, 261–270. <https://doi.org/10.1016/j.neuroimage.2011.06.094>, PubMed: 21763774
- Jung, T. P., Makeig, S., Westerfield, M., Townsend, J., Courchesne, E., & Sejnowski, T. J. (2000). Removal of eye activity artifacts from visual event-related potentials in normal and clinical subjects. *Clinical Neurophysiology*, 111, 1745–1758. [https://doi.org/10.1016/S1388-2457\(00\)00386-2](https://doi.org/10.1016/S1388-2457(00)00386-2), PubMed: 11018488
- Kałamała, P., Ociepka, M., & Chuderski, A. (2020). ERP evidence for rapid within-trial adaptation of cognitive control during conflict resolution. *Cortex*, 131, 151–163. <https://doi.org/10.1016/j.cortex.2020.07.012>, PubMed: 32861969
- Kerns, J. G., Cohen, J. D., MacDonald, A. W., III, Cho, R. Y., Stenger, V. A., & Carter, C. S. (2004). Anterior cingulate conflict monitoring and adjustments in control. *Science*, 303, 1023–1026. <https://doi.org/10.1126/science.1089910>, PubMed: 14963333

- Kim, S., & Cho, Y. S. (2014). Congruency sequence effect without feature integration and contingency learning. *Acta Psychologica*, 149, 60–68. <https://doi.org/10.1016/j.actpsy.2014.03.004>, PubMed: 24704781
- Kim, S., Lee, S. H., & Cho, Y. S. (2015). Control processes through the suppression of the automatic response activation triggered by task-irrelevant information in the Simon-type tasks. *Acta Psychologica*, 162, 51–61. <https://doi.org/10.1016/j.actpsy.2015.10.001>, PubMed: 26479902
- Koelewijn, T., van Schie, H. T., Bekkering, H., Oostenveld, R., & Jensen, O. (2008). Motor-cortical beta oscillations are modulated by correctness of observed action. *Neuroimage*, 40, 767–775. <https://doi.org/10.1016/j.neuroimage.2007.12.018>, PubMed: 18234516
- Koob, V., Mackenzie, I., Ulrich, R., Leuthold, H., & Janczyk, M. (2023). The role of task-relevant and task-irrelevant information in congruency sequence effects: Applying the diffusion model for conflict tasks. *Cognitive Psychology*, 140, 101528. <https://doi.org/10.1016/j.cogpsych.2022.101528>, PubMed: 36584549
- Kornblum, S., Hasbroucq, T., & Osman, A. (1990). Dimensional overlap: Cognitive basis for stimulus-response compatibility—A model and taxonomy. *Psychological Review*, 97, 253–270. <https://doi.org/10.1037/0033-295X.97.2.253>, PubMed: 2186425
- Larson, M. J., & Clayson, P. E. (2011). The relationship between cognitive performance and electrophysiological indices of performance monitoring. *Cognitive, Affective, & Behavioral Neuroscience*, 11, 159–171. <https://doi.org/10.3758/s13415-010-0018-6>, PubMed: 21264645
- Lee, J., & Cho, Y. S. (2013). Congruency sequence effect in cross-task context: Evidence for dimension-specific modulation. *Acta Psychologica*, 144, 617–627. <https://doi.org/10.1016/j.actpsy.2013.09.013>, PubMed: 24184348
- Lee, N., & Cho, Y. S. (2024). Investigating the nature of spatial codes for different modes of Simon tasks: Evidence from congruency sequence effects and delta functions. *Journal of Experimental Psychology: Human Perception and Performance*, 50, 819–841. <https://doi.org/10.1037/xhp0001220>, PubMed: 38900528
- Lee, Y. S., & Cho, Y. S. (2023). The congruency sequence effect of the Simon task in a cross-modality context. *Journal of Experimental Psychology: Human Perception and Performance*, 49, 1221–1235. <https://doi.org/10.1037/xhp0001145>, PubMed: 37410404
- Li, Q., Wang, K., Nan, W., Zheng, Y., Wu, H., Wang, H., et al. (2015). Electrophysiological dynamics reveal distinct processing of stimulus–stimulus and stimulus–response conflicts. *Psychophysiology*, 52, 562–571. <https://doi.org/10.1111/psyp.12382>, PubMed: 25395309
- Li, Q., Yin, S., Wang, J., Zhang, M., Li, Z., Chen, X., et al. (2023). Not all errors are created equal: Decoding the error-processing mechanisms using alpha oscillations. *Cerebral Cortex*, 33, 8110–8121. <https://doi.org/10.1093/cercor/bhd102>, PubMed: 36997156
- Lim, C. E., & Cho, Y. S. (2018). Determining the scope of control underlying the congruency sequence effect: Roles of stimulus–response mapping and response mode. *Acta Psychologica*, 190, 267–276. <https://doi.org/10.1016/j.actpsy.2018.08.012>, PubMed: 30170247
- Lim, C. E., & Cho, Y. S. (2021a). Cross-task congruency sequence effect without the contribution of multiple expectancy. *Acta Psychologica*, 214, 103268. <https://doi.org/10.1016/j.actpsy.2021.103268>, PubMed: 33609972
- Lim, C. E., & Cho, Y. S. (2021b). Response mode modulates the congruency sequence effect in spatial conflict tasks: Evidence from aimed-movement responses. *Psychological Research*, 85, 2047–2068. <https://doi.org/10.1007/s00426-020-01376-3>, PubMed: 32592067
- Lopez-Calderon, J., & Luck, S. J. (2014). ERPLAB: An open-source toolbox for the analysis of event-related potentials. *Frontiers in Human Neuroscience*, 8, 213. <https://doi.org/10.3389/fnhum.2014.00213>, PubMed: 24782741
- Luck, S. J. (2012). *Event-related potentials*. Oxford University Press. <https://doi.org/10.1037/13619-028>
- Luck, S. J. (2014). *An introduction to the event-related potential technique* (2nd ed.). MIT Press.
- MacDonald, A. W., III, Cohen, J. D., Stenger, V. A., & Carter, C. S. (2000). Dissociating the role of the dorsolateral prefrontal and anterior cingulate cortex in cognitive control. *Science*, 288, 1835–1838. <https://doi.org/10.1126/science.288.5472.1835>, PubMed: 10846167
- Maris, E., & Oostenveld, R. (2007). Nonparametric statistical testing of EEG- and MEG-data. *Journal of Neuroscience Methods*, 164, 177–190. <https://doi.org/10.1016/j.jneumeth.2007.03.024>, PubMed: 17517438
- Mayr, U., Awh, E., & Laurey, P. (2003). Conflict adaptation effects in the absence of executive control. *Nature Neuroscience*, 6, 450–452. <https://doi.org/10.1038/nn1051>, PubMed: 12704394
- Miyake, A., Friedman, N. P., Emerson, M. J., Witzki, A. H., Howerter, A., & Wager, T. D. (2000). The unity and diversity of executive functions and their contributions to complex “frontal lobe” tasks: A latent variable analysis. *Cognitive Psychology*, 41, 49–100. <https://doi.org/10.1006/cogp.1999.0734>, PubMed: 10945922
- Munakata, Y., Herd, S. A., Chatham, C. H., Depue, B. E., Banich, M. T., & O'Reilly, R. C. (2011). A unified framework for inhibitory control. *Trends in Cognitive Sciences*, 15, 453–459. <https://doi.org/10.1016/j.tics.2011.07.011>, PubMed: 21889391
- Nichols, T. E., & Holmes, A. P. (2002). Nonparametric permutation tests for functional neuroimaging: A primer with examples. *Human Brain Mapping*, 15, 1–25. <https://doi.org/10.1002/hbm.1058>, PubMed: 11747097
- Notebaert, W., Gevers, W., Verbruggen, F., & Liefoghe, B. (2006). Top-down and bottom-up sequential modulations of congruency effects. *Psychonomic Bulletin & Review*, 13, 112–117. <https://doi.org/10.3758/bf03193821>, PubMed: 16724777
- Notebaert, W., & Verguts, T. (2008). Cognitive control acts locally. *Cognition*, 106, 1071–1080. <https://doi.org/10.1016/j.cognition.2007.04.011>, PubMed: 17537419
- Nyhus, E., & Curran, T. (2010). Functional role of gamma and theta oscillations in episodic memory. *Neuroscience & Biobehavioral Reviews*, 34, 1023–1035. <https://doi.org/10.1016/j.neubiorev.2009.12.014>, PubMed: 20060015
- Palmer, C. E., Auksztulewicz, R., Ondobaka, S., & Kilner, J. M. (2019). Sensorimotor beta power reflects the precision-weighting afforded to sensory prediction errors. *Neuroimage*, 200, 59–71. <https://doi.org/10.1016/j.neuroimage.2019.06.034>, PubMed: 31226494
- Park, H.-D., Correia, S., Ducorps, A., & Tallon-Baudry, C. (2014). Spontaneous fluctuations in neural responses to heartbeats predict visual detection. *Nature Neuroscience*, 17, 612–618. <https://doi.org/10.1038/nn.3671>, PubMed: 24609466
- Pashler, H. (1997). *The psychology of attention*. MIT Press. <https://doi.org/10.7551/mitpress/5677.001.0001>
- Pastötter, B., Dreisbach, G., & Bäuml, K.-H. T. (2013). Dynamic adjustments of cognitive control: Oscillatory correlates of the conflict adaptation effect. *Journal of Cognitive Neuroscience*, 25, 2167–2178. https://doi.org/10.1162/jocn_a_00474, PubMed: 24001006
- Pavlidou, A., Schnitzler, A., & Lange, J. (2014). Beta oscillations and their functional role in movement perception.

- Translational Neuroscience*, 5, 286–292. <https://doi.org/10.2478/s13380-014-0236-4>
- Peylo, C., Hilla, Y., & Sauseng, P. (2021). Cause or consequence? Alpha oscillations in visuospatial attention. *Trends in Neurosciences*, 44, 705–713. <https://doi.org/10.1016/j.tins.2021.05.004>, PubMed: 34167840
- Pfurtscheller, G., Stancak, A., Jr., & Neuper, C. (1996). Post-movement beta synchronization. A correlate of an idling motor area? *Electroencephalography and Clinical Neurophysiology*, 98, 281–293. [https://doi.org/10.1016/0013-4694\(95\)00258-8](https://doi.org/10.1016/0013-4694(95)00258-8), PubMed: 8641150
- Purmann, S., & Pollmann, S. (2015). Adaptation to recent conflict in the classical color-word Stroop-task mainly involves facilitation of processing of task-relevant information. *Frontiers in Human Neuroscience*, 9, 88. <https://doi.org/10.3389/fnhum.2015.00088>, PubMed: 25784868
- Resulaj, A., Kiani, R., Wolpert, D. M., & Shadlen, M. N. (2009). Changes of mind in decision-making. *Nature*, 461, 263–266. <https://doi.org/10.1038/nature08275>, PubMed: 19693010
- Rey-Mermet, A., Gade, M., & Steinbauer, M. (2019). Sequential conflict resolution under multiple concurrent conflicts: An ERP study. *Neuroimage*, 188, 411–418. <https://doi.org/10.1016/j.neuroimage.2018.12.031>, PubMed: 30562575
- Riddle, J., Scimeca, J. M., Cellier, D., Dhanani, S., & D'Esposito, M. (2020). Causal evidence for a role of theta and alpha oscillations in the control of working memory. *Current Biology*, 30, 1748–1754. <https://doi.org/10.1016/j.cub.2020.02.065>, PubMed: 32275881
- Rubichi, S., & Pellicano, A. (2004). Does the Simon effect affect movement execution? *European Journal of Cognitive Psychology*, 16, 825–840. <https://doi.org/10.1080/09541440340000367>
- Schmidt, J. R., & De Houwer, J. (2011). Now you see it, now you don't: Controlling for contingencies and stimulus repetitions eliminates the Gratton effect. *Acta Psychologica*, 138, 176–186. <https://doi.org/10.1016/j.actpsy.2011.06.002>, PubMed: 21745649
- Schmidt, J. R., & Weissman, D. H. (2014). Congruency sequence effects without feature integration or contingency learning confounds. *PLoS One*, 9, e102337. <https://doi.org/10.1371/journal.pone.0102337>, PubMed: 25019526
- Schmidt, R., Ruiz, M. H., Kilavik, B. E., Lundqvist, M., Starr, P. A., & Aron, A. R. (2019). Beta oscillations in working memory, executive control of movement and thought, and sensorimotor function. *Journal of Neuroscience*, 39, 8231–8238. <https://doi.org/10.1523/JNEUROSCI.1163-19.2019>, PubMed: 31619492
- Schneider, D., Herbst, S. K., Klatt, L.-I., & Wöstmann, M. (2022). Target enhancement or distractor suppression? Functionally distinct alpha oscillations form the basis of attention. *European Journal of Neuroscience*, 55, 3256–3265. <https://doi.org/10.1111/ejn.15309>, PubMed: 33973310
- Smith, G. A., & Carew, M. (1987). Decision time unmasked: Individuals adopt different strategies. *Australian Journal of Psychology*, 39, 339–351. <https://doi.org/10.1080/00049538708259058>
- Soutschek, A., Müller, H. J., & Schubert, T. (2013). Conflict-specific effects of accessory stimuli on cognitive control in the Stroop task and the Simon task. *Experimental Psychology*, 60, 140–147. <https://doi.org/10.1027/1618-3169/a000181>, PubMed: 23128585
- Spapé, M. M., Band, G. P. H., & Hommel, B. (2011). Compatibility-sequence effects in the Simon task reflect episodic retrieval but not conflict adaptation: Evidence from LRP and N2. *Biological Psychology*, 88, 116–123. <https://doi.org/10.1016/j.biopsych.2011.07.001>, PubMed: 21767598
- Spitzer, B., & Haegens, S. (2017). Beyond the status quo: A role for beta oscillations in endogenous content (re)activation. *eNeuro*, 4, ENEURO.0170-17.2017. <https://doi.org/10.1523/eneuro.0170-17.2017>, PubMed: 28785729
- Stürmer, B., Leuthold, H., Soetens, E., Schröter, H., & Sommer, W. (2002). Control over location-based response activation in the Simon task: Behavioral and electrophysiological evidence. *Journal of Experimental Psychology: Human Perception and Performance*, 28, 1345–1363. <https://doi.org/10.1037/0096-1523.28.6.1345>, PubMed: 12542132
- Swann, N. C., Cai, W., Conner, C. R., Pieters, T. A., Claffey, M. P., George, J. S., et al. (2012). Roles for the pre-supplementary motor area and the right inferior frontal gyrus in stopping action: Electrophysiological responses and functional and structural connectivity. *Neuroimage*, 59, 2860–2870. <https://doi.org/10.1016/j.neuroimage.2011.09.049>, PubMed: 21979383
- Swann, N., Tandon, N., Canolty, R., Ellmore, T. M., McEvoy, L. K., Dreyer, S., et al. (2009). Intracranial EEG reveals a time- and frequency-specific role for the right inferior frontal gyrus and primary motor cortex in stopping initiated responses. *Journal of Neuroscience*, 29, 12675–12685. <https://doi.org/10.1523/JNEUROSCI.3359-09.2009>, PubMed: 19812342
- Tang, D., Hu, L., & Chen, A. (2013). The neural oscillations of conflict adaptation in the human frontal region. *Biological Psychology*, 93, 364–372. <https://doi.org/10.1016/j.biopsych.2013.03.004>, PubMed: 23570676
- Thut, G., Nietzel, A., Brandt, S. A., & Pascual-Leone, A. (2006). α -Band electroencephalographic activity over occipital cortex indexes visuospatial attention bias and predicts visual target detection. *Journal of Neuroscience*, 26, 9494–9502. <https://doi.org/10.1523/JNEUROSCI.0875-06.2006>, PubMed: 16971533
- Töllner, T., Wang, Y., Makeig, S., Müller, H. J., Jung, T.-P., & Gramann, K. (2017). Two independent frontal midline theta oscillations during conflict detection and adaptation in a Simon-type manual reaching task. *Journal of Neuroscience*, 37, 2504–2515. <https://doi.org/10.1523/JNEUROSCI.1752-16.2017>, PubMed: 28137968
- Van Diepen, R. M., Foxe, J. J., & Mazaheri, A. (2019). The functional role of alpha-band activity in attentional processing: The current zeitgeist and future outlook. *Current Opinion in Psychology*, 29, 229–238. <https://doi.org/10.1016/j.copsyc.2019.03.015>, PubMed: 31100655
- van Driel, J., Ort, E., Fahrenfort, J. J., & Olivers, C. N. L. (2019). Beta and theta oscillations differentially support free versus forced control over multiple-target search. *Journal of Neuroscience*, 39, 1733–1743. <https://doi.org/10.1523/JNEUROSCI.2547-18.2018>, PubMed: 30617208
- van Driel, J., Ridderinkhof, K. R., & Cohen, M. X. (2012). Not all errors are alike: Theta and alpha EEG dynamics relate to differences in error-processing dynamics. *Journal of Neuroscience*, 32, 16795–16806. <https://doi.org/10.1523/JNEUROSCI.0802-12.2012>, PubMed: 23175833
- van Driel, J., Sligte, I. G., Linders, J., Elport, D., & Cohen, M. X. (2015). Frequency band-specific electrical brain stimulation modulates cognitive control processes. *PLoS One*, 10, e0138984. <https://doi.org/10.1371/journal.pone.0138984>, PubMed: 26405801
- van Es, M. W. J., Gross, J., & Schoffelen, J.-M. (2020). Investigating the effects of pre-stimulus cortical oscillatory activity on behavior. *Neuroimage*, 223, 117351. <https://doi.org/10.1016/j.neuroimage.2020.117351>, PubMed: 32898680
- Wang, L., Chang, W., Krebs, R. M., Boehler, C. N., Theeuwes, J., & Zhou, X. (2019). Neural dynamics of reward-induced response activation and inhibition. *Cerebral Cortex*, 29,

- 3961–3976. <https://doi.org/10.1093/cercor/bhy275>, PubMed: 30365036
- Wang, X., Du, F., Hopfinger, J. B., & Zhang, K. (2018). Impaired conflict monitoring near the hands: Neurophysiological evidence. *Biological Psychology*, *138*, 41–47. <https://doi.org/10.1016/j.biopsych.2018.08.008>, PubMed: 30121288
- Wang, X.-J. (2010). Neurophysiological and computational principles of cortical rhythms in cognition. *Physiological Reviews*, *90*, 1195–1268. <https://doi.org/10.1152/physrev.00035.2008>, PubMed: 20664082
- Weissman, D. H., Hawks, Z. W., & Egner, T. (2016). Different levels of learning interact to shape the congruency sequence effect. *Journal of Experimental Psychology: Learning, Memory, and Cognition*, *42*, 566–583. <https://doi.org/10.1037/xlm0000182>, PubMed: 26389630
- Wiesman, A. I., Koshy, S. M., Heinrichs-Graham, E., & Wilson, T. W. (2020). Beta and gamma oscillations index cognitive interference effects across a distributed motor network. *Neuroimage*, *213*, 116747. <https://doi.org/10.1016/j.neuroimage.2020.116747>, PubMed: 32179103
- Yang, G., Nan, W., Zheng, Y., Wu, H., Li, Q., & Liu, X. (2017). Distinct cognitive control mechanisms as revealed by modality-specific conflict adaptation effects. *Journal of Experimental Psychology: Human Perception and Performance*, *43*, 807–818. <https://doi.org/10.1037/xhp0000351>, PubMed: 28345947
- Ye, W., & Damian, M. F. (2023). Effects of conflict in cognitive control: Evidence from mouse tracking. *Quarterly Journal of Experimental Psychology*, *76*, 54–69. <https://doi.org/10.1177/1747021822107826>, PubMed: 35045771